Research article

JGS
Journal of the Geological Society

https://doi.org/10.1144/jgs2020-163 | Vol. 178 | 2020 | jgs2020-163

Stable isotopes ($\delta^{13}C$, $\delta^{18}O$) and element ratios (Mg/Ca, Sr/Ca) of Jurassic belemnites, bivalves and brachiopods from the Neuquén Basin (Argentina): challenges and opportunities for palaeoenvironmental reconstructions

Matthias Alberti[1*], Horacio Parent[2], Alberto C. Garrido[3,4], Nils Andersen[5], Dieter Garbe-Schönberg[1] and Silvia Danise[6]

[1] Institut für Geowissenschaften, Christian-Albrechts-Universität zu Kiel, Ludewig-Meyn-Straße 10, 24118 Kiel, Germany
[2] Laboratorio de Paleontología, IFG-FCEIA, Universidad Nacional de Rosario, Pellegrini 250, 2000 Rosario, Argentina
[3] Museo Provincial de Ciencias Naturales 'Prof. Dr. Juan Olsacher', Dirección Provincial de Minería, Elena de Vega 472, 8340 Zapala, Argentina
[4] Centro de Investigación en Geociencias de la Patagonia – CIGPat, Departamento de Geología y Petróleo, Facultad de Ingeniería, Universidad Nacional del Comahue, Buenos Aires 1400, Neuquén, Argentina
[5] Leibniz Laboratory for Radiometric Dating and Stable Isotope Research, Christian-Albrechts-Universität zu Kiel, Max-Eyth-Straße 11, 24118 Kiel, Germany
[6] Dipartimento di Scienze della Terra, Università degli Studi di Firenze, Via La Pira 4, 50121, Firenze, Italy
MA, 0000-0003-1094-8885; NA, 0000-0003-4148-6791; DG-S, 0000-0001-9006-9463; SD, 0000-0002-6098-609X
* Correspondence: matthias.alberti@ifg.uni-kiel.de

Abstract: Fossils from the Jurassic succession of the Neuquén Basin (Argentina) were analysed for their stable isotope ($\delta^{13}C$, $\delta^{18}O$) and elemental (Mg/Ca, Sr/Ca) composition. Mg/Ca ratios point to comparatively stable temperature conditions from the Bajocian to Early Oxfordian and during the Tithonian, but do not allow a reliable reconstruction of absolute water temperatures. Sr/Ca ratios follow the general global pattern, indicating water exchange between the basin and the open ocean. The $\delta^{18}O$ values can be translated into water temperatures between 20 and 25°C for most of the studied intervals with possible shorter cold spells in the Late Pliensbachian, Bajocian and Late Tithonian. However, precise temperature reconstructions are complicated by bivalve shells from the northern–central part of the basin pointing to local fluctuations in the $\delta^{18}O$ values of seawater. Potential reasons for these variations are discussed, but it seems most likely that they are caused by phases of enhanced freshwater input leading to meso- to brachyhaline conditions in the northern study areas. This paper therefore exemplifies the particular challenges for temperature reconstructions in marginal seas and highlights the opportunities of combining different geochemical proxies to disentangle the influence of different environmental parameters.

Supplementary material: Detailed results of the geochemical analyses, geographical coordinates and information on biostratigraphy are available at https://doi.org/10.6084/m9.figshare.c.5173466

Received 31 August 2020; **revised** 10 October 2020; **accepted** 12 October 2020

Over recent decades, stable oxygen isotope analyses of fossil hardparts ($\delta^{18}O_{shell}$) have been used to continuously improve our understanding of the Jurassic world and climate (e.g. Bowen 1963; Stevens and Clayton 1971; Ditchfield *et al.* 1994; Price and Sellwood 1997; Dromart *et al.* 2003; Dera *et al.* 2011; Korte *et al.* 2015). Nevertheless, such studies focusing mainly on the reconstruction of water temperatures are still dominated by data for European localities, with other regions being comparatively understudied. To differentiate between global and regional trends, data from other regions are necessary. The present study concentrates on the Jurassic of Argentina and is part of a series of papers aimed at deepening our understanding of environmental conditions of Gondwanan localities (Alberti *et al.* 2012*a*, *b*, 2013, 2017, 2019*a*, *b*, 2020).

South America has extensive Jurassic successions, which have been studied by geoscientists for considerable time (e.g. pioneer studies by Steuer 1897; Burckhardt 1900, 1903; Haupt 1907; Weaver 1931). Their rich fossil content has sparked various palaeontological studies and also allowed the establishment of a biostratigraphic framework based on ammonites with an ever-increasing resolution. Although well-preserved fossils are common in many stratigraphic intervals, attempts at reconstructing environmental conditions during the Jurassic based on geochemical analyses of well-dated shells are still few (e.g. Bowen 1963; Volkheimer *et al.* 2008; Gómez-Dacal *et al.* 2018; Alberti *et al.* 2019*b*). Temperature reconstructions based on $\delta^{18}O_{shell}$ analyses in particular necessitate assumptions on the depositional setting including water depth or the $\delta^{18}O$ value of seawater ($\delta^{18}O_{sea}$) during the lifetime of the analysed fossil organisms. Influences such as evaporation, river discharge or rainfall patterns are particularly important for marginal seas such as the Neuquén Basin, which was separated from the open ocean by a volcanic arc (Fig. 1; compare Lazo *et al.* 2008). To differentiate environmental parameters, the present study combines the analyses of stable isotopes ($\delta^{18}O$, $\delta^{13}C$) and element ratios (Mg/Ca, Sr/Ca) of 179 fossil specimens from the Neuquén Basin. Elemental analyses (Fe, Mn) were also used to evaluate the preservational quality of the studied fossils.

Geological overview

The Neuquén Basin is situated between 34 and 41°S and 66 and 71°W in southwestern South America, covering *c.* 120 000 km^2 of present-day Chile and Argentina (Fig. 2; Howell *et al.* 2005; Parent *et al.* 2013). The Triassic–Paleogene succession consists of several

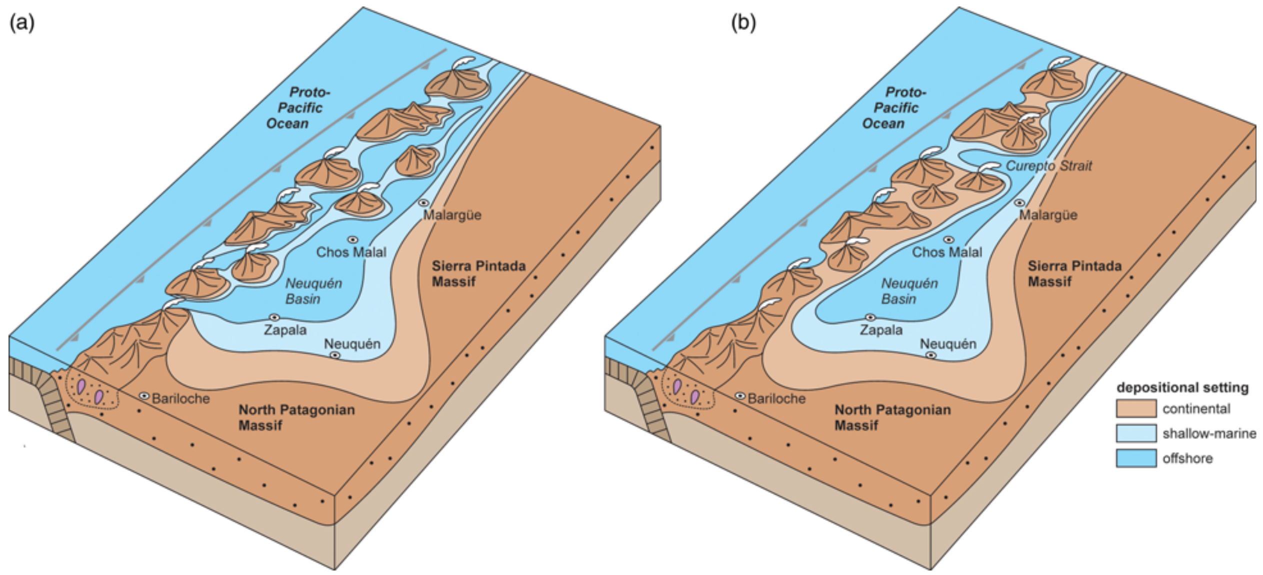

Fig. 1. Palaeogeographical reconstructions for the Neuquén Basin during the Jurassic (modified after Howell *et al.* 2005). It is still debated whether the volcanic arc separating the basin from the open ocean consisted of a chain of individual islands (**a**; Howell *et al.* 2005) or constituted a continuous landmass pierced by only one seaway (**b**; Vicente 2005). The study areas are around Zapala (southern sections) and Chos Malal (northern sections).

thousand metres of sedimentary rocks including an almost complete Jurassic–Early Cretaceous marine record (Howell *et al.* 2005). During most of its development and at present, the Neuquén Basin is delimited by the Sierra Pintada Massif in the NE and the North Patagonian Massif in the south, while the Andean volcanic arc separates the basin from the open Pacific Ocean (Fig. 1). It is unknown to what degree water exchange with the open ocean was possible or where exactly seaways for such an exchange existed. Some reconstructions depict the volcanic arc as a loose chain of islands (e.g. Howell *et al.* 2005; Fig. 1a). In contrast, Vicente (2005) proposed a more restricted situation with a single connection north of the basin (i.e. the Curepto Strait; Fig. 1b). Eventually, the continued Andean orogeny led to the uplift and folding of the Mesozoic strata, which became subsequently exposed in the western part of the Neuquén Basin (Howell *et al.* 2005).

The material used in the present study has been collected from two groups of outcrops: (1) the northern sections in the vicinity of Chos Malal; (2) the southern sections near Zapala (Fig. 2). The two areas are *c.* 180 km apart and characterized by slightly different depositional settings (Fig. 3). The northern sections near Chos Malal include the localities of Vega de la Veranada (VV) and Pampa Tril (PT). Studied outcrops in this area include Bajocian to lower Cretaceous rocks with marine fossils occurring at several levels. In the Bathonian to Oxfordian strata, bivalves occur regularly, whereas belemnites and ammonites become more common in the Tithonian. Ammonites allow precise age assignments for large parts of the succession (compare Parent and Garrido 2015; Parent *et al.* 2015, 2020). In general, siliciclastic rocks (partly cross-bedded) dominate the Middle Jurassic, but the Upper Callovian to Oxfordian La Manga Formation is characterized by carbonates interpreted as a distal platform (Gulisano 1992). The Middle Oxfordian to Kimmeridgian strata consist of massive evaporites and continental rocks. The Tithonian to lowermost Cretaceous units are again dominated by fine-grained siliciclastic deposits, which were interpreted as basinal to outer ramp deposits (e.g. Spalletti *et al.* 1999). Finally, the Lower Valanginian Mulichinco Formation

Fig. 2. Schematic map of the study area in the Neuquén Basin (shaded) in southwestern South America showing the location of the studied sections near Chos Malal in the north and Zapala in the south.

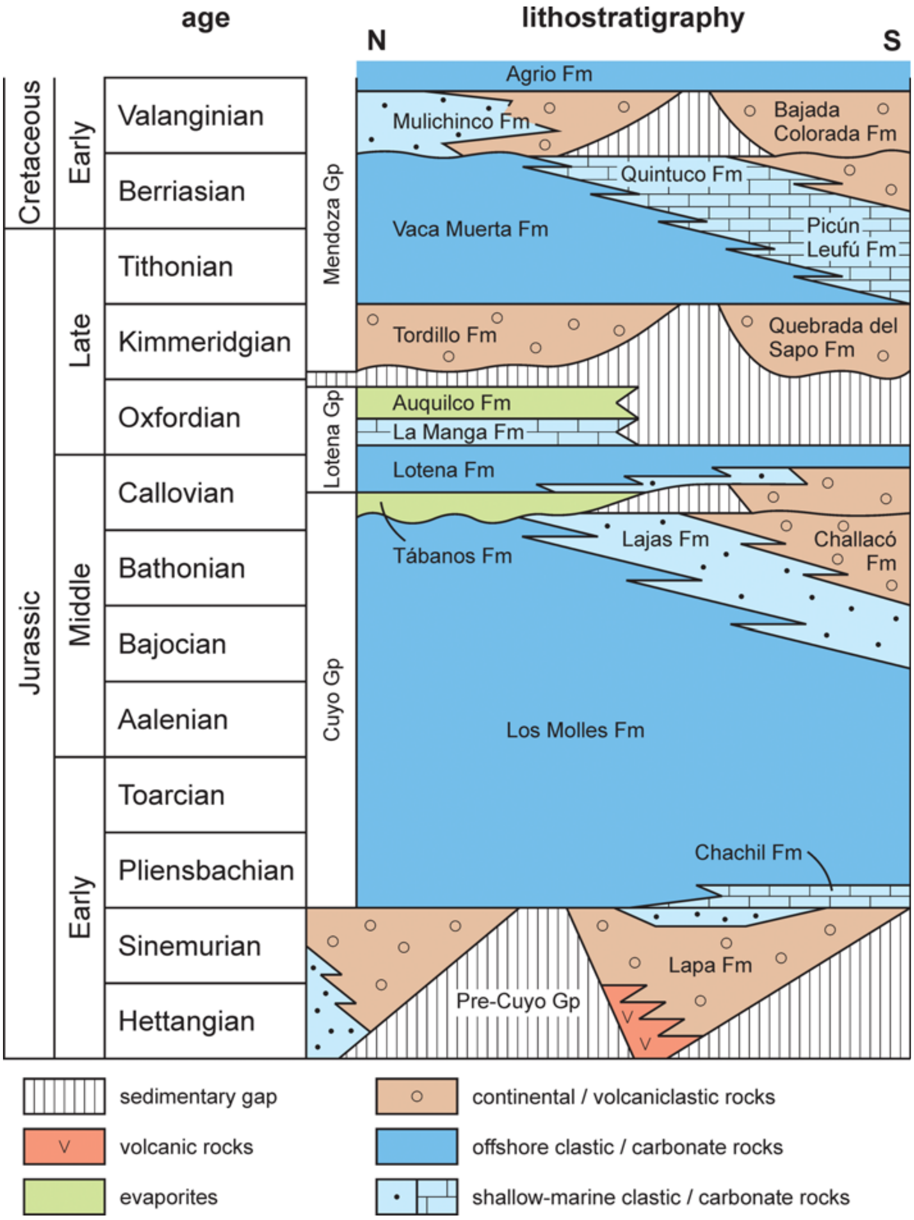

Fig. 3. General lithostratigraphic framework and major facies types for the Jurassic and Lower Cretaceous of the Neuquén Basin (modified after Howell *et al.* 2005).

consists of calcareous sandstones with oysters (Schwarz and Howell 2005).

The following sections were sampled near Zapala in the southern Neuquén Basin: Portada Covunco (PC), Cerrito Caracoles (CC), Cerro Granito (CG), Picún Leufú (PL-1&2), Picún Leufú Campamento Vialidad (PL-CV) and Charahuilla (CH). Some of these localities represent classic sections studied for many decades (e.g. Suero 1951; Westermann and Riccardi 1979; Leanza 1990, 1993; Leanza *et al.* 2013). In general, the depositional setting in the southern Neuquén Basin has been described as more shallow than further north owing to the Huincul Arch (compare Parent *et al.* 2013). Consequently, the fossil fauna is often more diverse, including bivalves, ammonites, brachiopods, gastropods, echinoderms, hermatypic corals and serpulids (e.g. Armella *et al.* 2007, 2008; Garrido and Parent 2013; Parent *et al.* 2013). The succession is dominated by marine siliciclastic deposits with intercalations of continental rocks (e.g. in the Callovian and Kimmeridgian; Fig. 3). A noteworthy exception is the Tithonian Picún Leufú Formation, which consists of bioclastic limestones in addition to calcareous siltstones. The individual localities and sections are described in more detail in the Supplementary material (including geographical coordinates and information on biostratigraphy).

Material and methods

In total, 119 bivalves, 50 belemnites, seven brachiopods and three aptychi were analysed in the present study (for photographs of exemplary specimens see the Supplementary material). Most of these fossils were collected during a field survey in February 2018 at the localities of Vega de la Veranada, Pampa Tril and Picún Leufú 1. Additional shells were selected from the collections of the Museo Provincial de Ciencias Naturales ‘Prof. Dr. Juan A. Olsacher’ in Zapala, Argentina. The vast majority of the selected shells are oysters belonging to the genus *Gryphaea*. In addition, few shells of *Actinostreon*?, *Aetostreon*, *Placunopsis*? and *Trichites* were analysed (for bivalve taxonomy see Aberhan 1994; Rubilar 2005; Lazo 2007; Rubilar and Lazo 2009; Bressan and Palma 2010). Jurassic belemnites of the Neuquén Basin are still relatively poorly known. The majority of the Bajocian rostra have a short conical form without a groove and could be assigned to the genus *Brevibelus*. The Callovian–Oxfordian specimens are characterized by a depressed cross-section with a prominent ventral groove and can be assigned to the genus *Belemnopsis*. The Tithonian belemnites belonging to the genus *Hibolithes* show mostly elongate rostra, which are cylindrical in cross-section and have no or only a weak shallow ventral groove (for belemnite taxonomy see Howlett 1989; Doyle 1992; Doyle *et al.* 1996, 1997). Analysed brachiopods were identified as the rhynchonellid species *Rhynchonelloides lamberti*, *Piarorhynchia keideli* and *Rhynchonella variabilis*. Because of occasional fragmentary preservation, not all collected fossils could be identified to generic level.

Most of the collected fossils can be attributed to a particular horizon and ammonite zone in previously published sections (see Supplementary material for details). The individual sections were correlated based on regional and Tethyan ammonite biostratigraphy and 'theoretical' numerical ages were assigned to each sample based on the Geological Time Scale 2016 (Ogg *et al.* 2016). This age model is theoretical to the extent that dating and correlating of ammonite zones in South America are continuing processes and continuous changes are expected in the future (e.g. Lena *et al.* 2019). Even though such changes and improvements in dating might change the assigned numerical ages of the samples, the overall trends discussed in the present study will probably remain the same. The northern sections near Chos Malal are represented by samples from the Lower–Middle Bathonian to Lower Oxfordian and the Tithonian. Fossils of the southern sections near Zapala were collected from the Pliensbachian, Lower Bajocian, Bathonian and Tithonian. The sampling focus lay on Middle and Upper Jurassic sections, but no fossils could be collected from the Middle Oxfordian to Kimmeridgian interval, as the corresponding strata consist of continental to evaporitic deposits, which do not contain marine fossils (Fig. 3).

The collected fossils were examined macroscopically and the seemingly best preserved specimens were subsequently cleaned and sampled with a hand-held dental drill. For bivalves and brachiopods, the areas close to the umbo/hinge and near muscle scars were avoided, as these are often influenced by vital effects during shell formation (e.g. Carpenter and Lohmann 1995). Similarly, belemnite rostra were not sampled close to the outer rim or near the alveole, as these are commonly prone to alteration. Large oyster shells were rare, but one specimen of *Gryphaea* sp. from the Lower Oxfordian could be cut longitudinally and sampled at high resolution, with 27 samples taken along a transect perpendicular to the growth lines. In addition, five samples of sediment and one sample of cement filling the alveole of a belemnite rostrum were collected. All specimens are permanently stored at the Museo Provincial de Ciencias Naturales 'Prof. Dr. Juan A. Olsacher' in Zapala, Argentina.

The collected carbonate powder was analysed using a carbonate preparation device (Kiel IV) connected to a ThermoScientific MAT 253 mass spectrometer at the Leibniz Laboratory for Radiometric Dating and Stable Isotope Research at the Christian-Albrechts-Universität zu Kiel, Germany. The carbonate samples were reacted within the preparation device with 100% orthophosphoric acid at 75°C and the evolved CO_2 gas was then analysed using the mass spectrometer. On daily routine, different laboratory internal carbonate standards and two international carbonate standards (NBS-19; IAEA-603) were analysed to control the precision of measured $\delta^{13}C$ and $\delta^{18}O$ values. All values are reported in per mil relative to the Vienna Pee Dee Belemnite (VPDB) scale using NBS-19. Analytical precision of stable isotope analysis was better than ±0.08‰ (±1SD) for $\delta^{18}O$ and better than ±0.05‰ (±1SD) for $\delta^{13}C$.

In most cases, the sample size was large enough for elemental analyses in addition to stable isotope analyses. Samples were dissolved in dilute nitric acid and analysed for their Mg/Ca and Sr/Ca ratios and Fe, Mn mass fractions by inductively coupled plasma optical emission spectrometry using a Spectro Ciros SOP instrument at the Institut für Geowissenschaften, Christian-Albrechts-Universität zu Kiel, Germany. Average uncertainty for Sr/Ca was around 0.9‰ and for Mg/Ca around 1.2‰. Reference materials Coral JCp-1, Tridacna JCt-1 and carbonate ECRM 752 were used as secondary standards.

Within the present study, potential correlations between different analytical results in the acquired datasets were evaluated with the help of the Spearman correlation coefficient (rs). Illustrated linear trend lines are based on reduced major axis (RMA) regression.

Results

Detailed results of the geochemical analyses are listed in the Supplementary material.

Preservation of the fossil material

A thorough check of the preservational quality is very important in any study using fossil shells for geochemical analyses. Cathodoluminescence microscopy has become a standard procedure to examine whether diagenetic alteration changed the chemical composition of fossil shells (e.g. Wierzbowski 2002, 2004; Wierzbowski and Joachimski 2007; Ullmann and Korte 2015; Arabas 2016; Arabas *et al.* 2017), but unfortunately such an easy check was not possible in the current study as the fossil material had to remain in Argentina. Instead, iron and manganese contents were analysed for most of the used specimens, which also allow an evaluation of preservational quality (e.g. Brand and Veizer 1980, 1981; Price and Sellwood 1997; Wierzbowski and Joachimski 2007; Wierzbowski *et al.* 2009; Fujioka *et al.* 2019). Because concentrations of both elements are relatively low in pristine shells, cut-off values can be defined, which may be used to separate potentially altered samples from the database. Results from sediment and cement samples show high iron and manganese contents, thereby attesting to the availability of both elements in porewaters. Consequently, all fossils with an iron content above 300 $\mu g\ g^{-1}$ and a manganese content above 100 $\mu g\ g^{-1}$ were removed from environmental reconstructions (compare similar cut-off values used by Wierzbowski and Joachimski 2007; Wierzbowski *et al.* 2009; Nunn and Price 2010; Alberti *et al.* 2012*b*; Arabas *et al.* 2017). Furthermore, all specimens for which elemental analysis could not be performed were considered unreliable and excluded from further interpretations. Of the 119 sampled bivalves, 12 did not yield enough carbonate powder for elemental analysis and 47 were deemed unreliable because of exceeding the cut-off grades in their iron and/or manganese content. This left 60 presumably well-preserved bivalve shells. Of the 50 sampled belemnite rostra, 48 could be analysed for their element content. Five belemnite rostra were removed from further interpretations because of high iron and/or manganese contents. This left 43 seemingly well-preserved belemnites. Most of the collected brachiopods showed some abrasion on the outer shell surface. Owing to their thin inner shell layer, only two of the seven brachiopod shells yielded enough sample material for elemental analyses and both were considered well preserved. Finally, all three aptychi were deemed unreliable as their data reflect either diagenetically altered carbonate or contamination by carbonate cements filling the abundant pores in the shell plates. After elemental analyses, the collection was separated into seemingly well-preserved specimens and possibly unreliable fossils. Although both datasets are included in the Supplementary material, only results of the well-preserved fossils were used for interpretations.

Another potential indicator for the alteration of the stable isotope composition of fossil shells is a correlation of their $\delta^{18}O$ and $\delta^{13}C$ values (e.g. Hodgson 1966; Ullmann and Korte 2015). Although such a correlation can occasionally be primary in origin (e.g. owing to a stronger primary productivity at higher temperatures), diagenetic alteration commonly leads to a decrease in $\delta^{18}O$ and $\delta^{13}C$ values (e.g. Hodgson 1966; Hudson 1977; Nelson and Smith 1996). This can be demonstrated by the results from the sediment samples, which show much lower $\delta^{18}O$ and $\delta^{13}C$ values than well-preserved fossils. Similarly, several fossil shells, which were considered unreliable and potentially diagenetically altered because of their high iron and/or manganese contents, exhibit lowered $\delta^{18}O$ and $\delta^{13}C$ values (Fig. 4). Consequently, an increasing alteration of shells should lead to a positive correlation between the stable isotope values. In contrast, the 60 well-preserved bivalve shells show a negative correlation (rs = −0.60, $P < 0.05$) which is believed to be caused by the strong variation of analytical results between the different study areas instead of diagenetic alteration. If only the bivalves of the northern sections are considered, the negative correlation is weaker (rs = −0.44, $P < 0.05$; Fig. 4). The oysters of the southern sections show no significant correlation (rs = −0.16, $P = 0.58$; Fig. 4). Similarly, the $\delta^{18}O$ and $\delta^{13}C$ values of the 43 well-preserved belemnites show no significant correlation (rs = 0.00, $P = 0.97$; Fig. 4), also if separated by study area.

Results of stable isotope and element analyses

Because the results are markedly different between the northern and the southern sections, each will be described separately in the following paragraphs.

Northern sections near Chos Malal

The $\delta^{13}C$ values of well-preserved oyster shells near Chos Malal (Fig. 5a) show an increase from the Early–Middle Bathonian (average 2.09‰) to the Late Callovian (Dimorphosus Zone, average 3.83‰) and then a slight decrease into the Early Oxfordian (Pressulus Zone, average 3.31‰). No samples are available from the Kimmeridgian, but in the Early Tithonian $\delta^{13}C$ values are low (Picunleufuense Zone, average 0.91‰). Values then increase slightly towards the Middle Tithonian (Zitteli/Mendozanus Zone, average 1.74‰) and then decrease again until the Late Tithonian (Alternans Zone, minimum −0.33‰). The two oyster shells with a Valanginian age have again slightly higher $\delta^{13}C$ values (Riveroi Zone, average 1.10‰). The number of belemnites from the northern sections is comparatively limited, but the results show a similar pattern to the oysters, with higher $\delta^{13}C$ values in the Early Oxfordian (Pressulus Zone, average 0.57‰) and lower values in the Tithonian (average −1.11‰).

The $\delta^{18}O$ values of well-preserved Jurassic oyster shells of the northern sections (Fig. 5b) are all strikingly low (below −5‰). The

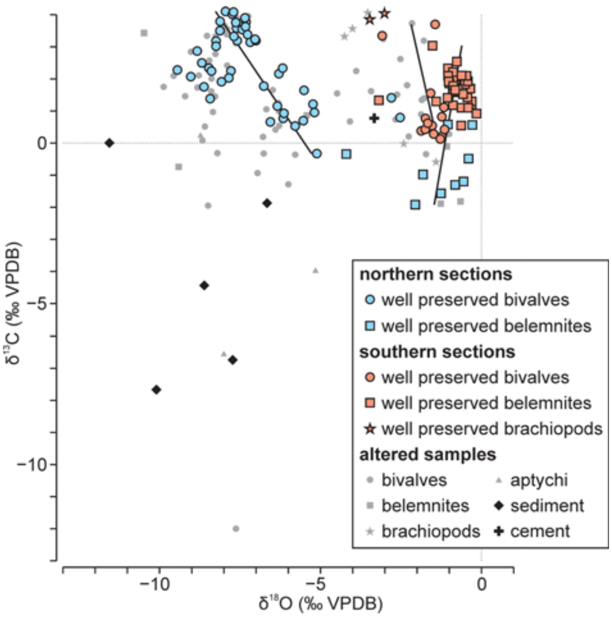

Fig. 4. $\delta^{18}O$ v. $\delta^{13}C$ values of fossils and sediment samples of the northern sections near Chos Malal and the southern sections near Zapala.

data show a gradual increase from the Early–Middle Bathonian (average −8.59‰) to the Early Oxfordian (Pressulus Zone, average −7.54‰). After a gap in data, this trend can be followed further from the Early Tithonian (Picunleufuense Zone, average −6.45‰) to the Late Tithonian (Alternans Zone, maximum −5.11‰). The two Valanginian oysters show much higher $\delta^{18}O$ values (Riveroi Zone, average −2.66‰). In contrast to the oysters, the belemnites of the northern sections show no characteristic trend through time, but much higher absolute values. In the Early Oxfordian (Pressulus Zone), $\delta^{18}O$ values of belemnites vary around an average of −0.67‰. In the Tithonian, values are again slightly lower (average −1.59‰) but also fairly scattered (between −4.20 and −0.40‰).

The Mg/Ca ratios of well-preserved oysters of the northern sections remain largely stable through time (Fig. 5c). The record begins in the Early–Middle Bathonian (average 2.42 mmol mol^{-1}) and changes little until the Early Oxfordian (Pressulus Zone, average 2.36 mmol mol^{-1}). Values are similar in the Early (Picunleufuense Zone, average 2.85 mmol mol^{-1}) and Middle Tithonian (Zitteli/Mendozanus Zone, average 2.13 mmol mol^{-1}; Internispinosum Zone, average 2.90 mmol mol^{-1}). Mg/Ca ratios in the Late Tithonian (Alternans Zone) fluctuate mostly around an average of 1.63 mmol mol^{-1}, except for one outlier with a Mg/Ca ratio of 8.16 mmol mol^{-1} (sample MOZ-PI 11834/1). The two oysters from the Valanginian (Riveroi Zone) have Mg/Ca ratios around an average of 2.51 mmol mol^{-1}. In comparison, the belemnites have much higher Mg/Ca ratios. The two specimens of the Early Oxfordian (Pressulus Zone) have values around an average of 8.52 mmol mol^{-1}. In the Tithonian, the ratios fluctuate strongly around an average of 11.35 mmol mol^{-1} (between 7.92 and 14.42 mmol mol^{-1}).

The Sr/Ca ratios of oyster shells (Fig. 5d) of the northern sections are relatively stable from the Early–Middle Bathonian (average 0.59 mmol mol^{-1}) to the early Late Callovian (Primus Zone, average 0.60 mmol mol^{-1}). Following this, the Sr/Ca ratio decreases and reaches lowest values in the Early Oxfordian (Pressulus Zone, average 0.46 mmol mol^{-1}). In the Tithonian, Sr/Ca ratios are generally higher and show an increase from the Early Tithonian (Picunleufuense Zone, average 0.75 mmol mol^{-1}) to the Middle Tithonian (Zitteli/Mendozanus Zone, average 1.07 mmol mol^{-1}) and a subsequent decrease until the Late Tithonian (Alternans Zone, minimum 0.73 mmol mol^{-1}). The two Valanginian (Riveroi Zone) oysters show Sr/Ca ratios around an average of 0.86 mmol mol^{-1}. The Sr/Ca ratios of belemnites of the Early Oxfordian (Pressulus Zone) vary around an average of 1.39 mmol mol^{-1}. In the Tithonian, the values fluctuate more strongly around an average of 1.78 mmol mol^{-1} (between 1.33 and 2.17 mmol mol^{-1}).

Southern sections near Zapala

Two well-preserved rhynchonellid brachiopod shells with a Pliensbachian age show $\delta^{13}C$ values around an average of 3.96‰ (Fig. 6a). A well-preserved Early Bajocian (Giebeli Zone) oyster shell has a $\delta^{13}C$ value of 3.70‰ (sample MOZ-PI 11830/1) and another oyster shell from the Bathonian has a $\delta^{13}C$ value of 3.35‰ (sample MOZ-PI 11254). Considerably more data are available from well-preserved oyster shells with a Late Tithonian (Alternans Zone) age, which show $\delta^{13}C$ values around an average of 0.61‰. Although the dataset is limited (especially for the Bajocian and Bathonian), the values seem to show an overall decrease in $\delta^{13}C$ values from the Middle to Late Jurassic, similar to the northern sections (Fig. 5a). In addition, the recorded absolute $\delta^{13}C$ values of oyster shells are similar between the northern and southern sections (particularly for the Late Tithonian where more data are available for both areas). The 34 well-preserved belemnites with an Early Bajocian age (Giebeli Zone) show $\delta^{13}C$ values between 0.55 and 3.04‰ (average 1.69‰).

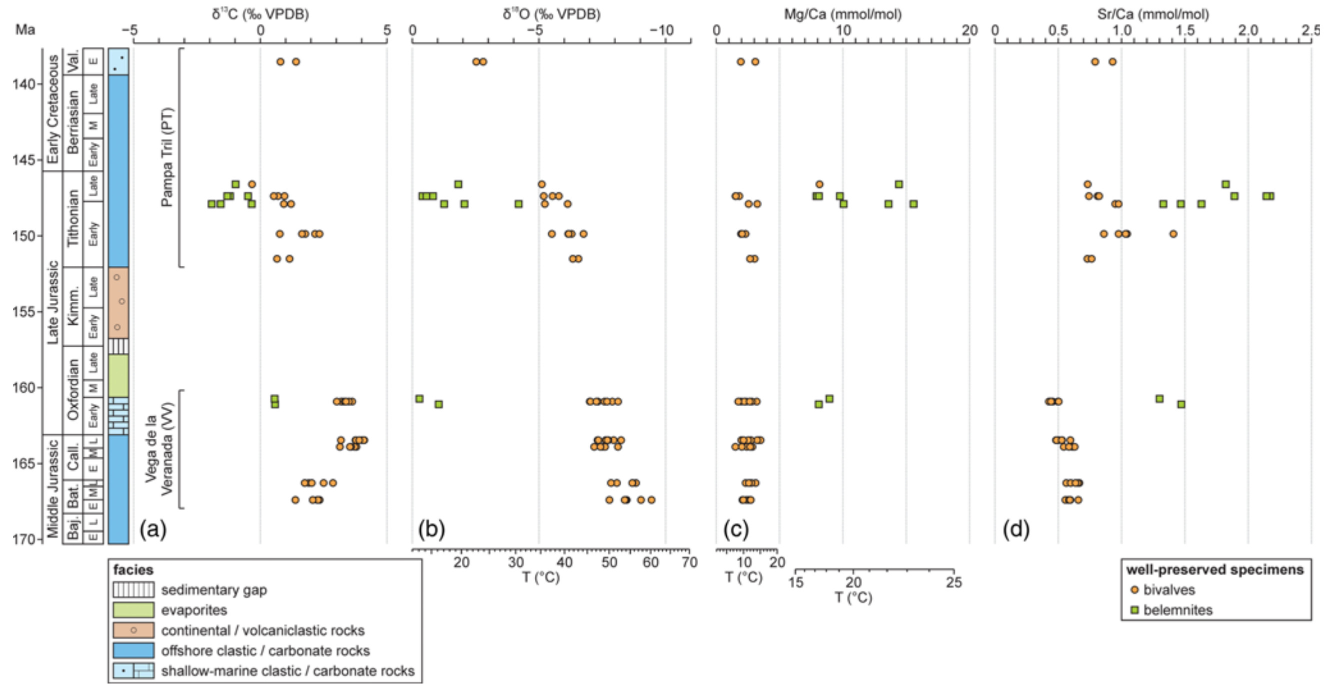

Fig. 5. Results of stable isotope ($\delta^{18}O$, $\delta^{13}C$) and element (Mg/Ca, Sr/Ca) analyses of well-preserved fossils of the northern sections near Chos Malal. Temperatures for $\delta^{18}O_{shell}$ values were reconstructed with the equation of Anderson and Arthur (1983) and a $\delta^{18}O_{sea}$ value of −1‰ for an ice-free Jurassic world as suggested by Shackleton and Kennett (1975). Temperatures for Mg/Ca ratios were calculated with the equations of Mouchi *et al.* (2013) for oysters and Nunn and Price (2010) for belemnites. Main facies types are based on Howell *et al.* (2005) and the age model is based on Ogg *et al.* (2016).

The $\delta^{18}O$ record starts with two rhynchonellid brachiopods of Pliensbachian age with values ranging around an average of −3.24‰ (Fig. 6b). Two well-preserved oysters from the Middle Jurassic give $\delta^{18}O$ values of −1.44‰ for the Early Bajocian (Giebeli Zone) and −3.08‰ for the Bathonian. The $\delta^{18}O$ values of oysters from the Late Tithonian (Alternans Zone) fluctuate around an average of −1.47‰. These values are much higher than those recorded from oysters of the northern sections. Furthermore, they do not show a very prominent trend through time. Belemnites of the Early Bajocian (Giebeli Zone) recorded $\delta^{18}O$ values between −1.52 and −0.16‰, except for one outlier with −3.19‰. Their overall average is −0.81‰, which is largely comparable with values of belemnites from the northern sections, although the latter have different ages.

The two brachiopods with a Pliensbachian age recorded Mg/Ca ratios with an average of 4.83 mmol mol^{-1} (Fig. 6c). The Mg/Ca ratios of well-preserved oysters are slightly lower but relatively stable through time. The oyster shells from the Early Bajocian (Giebeli Zone) and the Bathonian show Mg/Ca ratios of 2.10 mmol mol^{-1} and 2.41 mmol mol^{-1} respectively. In the Late Tithonian (Alternans Zone), Mg/Ca ratios of well-preserved oysters vary around an average of 2.91 mmol mol^{-1}. In general, the results are similar to those of oysters from the northern sections in absolute values and by being relatively stable through time. The belemnites with an Early Bajocian age (Giebeli Zone) show much higher Mg/Ca ratios around an average of 12.80 mmol mol^{-1} (ranging between 7.80 and 17.10 mmol mol^{-1}).

The two Pliensbachian brachiopod shells show Sr/Ca ratios around an average of 1.08 mmol mol^{-1} (Fig. 6d). The Sr/Ca ratios of well-preserved oyster shells seem relatively constant through time. Oysters from the Early Bajocian (Giebeli Zone) and the Bathonian have Sr/Ca ratios of around 0.72 mmol mol^{-1}. The Sr/Ca ratios of well-preserved bivalve shells from the Late Tithonian (Alternans Zone) fluctuate around an average of 0.71 mmol mol^{-1}. The belemnites with an Early Bajocian age (Giebeli Zone) have Sr/Ca ratios around an average of 1.58 mmol mol^{-1} (ranging between 1.38 and 1.80 mmol mol^{-1}).

Results of the high-resolution stable isotope analysis

One oyster shell (*Gryphaea* sp.) from the Lower Oxfordian (Pressulus Zone) of the Vega de la Veranada has been sampled at high resolution across growth layers *c.* 1 cm below the umbo (Fig. 7; Supplementary material). A total of 27 samples were taken with an average resolution of three samples per millimetre. These samples were analysed for their stable isotope composition. The $\delta^{18}O$ values show a cyclic nature around an average value of −7.06‰ with a maximum at −5.77‰ and a minimum at −8.33‰ (Fig. 7a). There are a total of three (possibly four) cycles visible in the $\delta^{18}O$ values, with the amplitude becoming increasingly weaker towards the younger side of the shell. The $\delta^{13}C$ values fluctuate less strongly around an average of 3.45‰ (maximum 3.79‰; minimum 3.09‰; Fig. 7b). They show a broad positive excursion in the older half of the shell and a broad negative excursion in the younger half. Overall, the $\delta^{18}O$ and $\delta^{13}C$ values show a weak correlation (rs = 0.45; P = 0.02; Fig. 7c).

Discussion

Differences between water temperature proxies

Several geochemical methods have been developed and applied to reconstruct absolute water temperatures in Earth's history including the Jurassic (e.g. Epstein *et al.* 1951; Urey *et al.* 1951; McArthur *et al.* 2007; Jenkyns *et al.* 2012; Li *et al.* 2013; Wierzbowski *et al.* 2018; Vickers *et al.* 2019). Among these, stable isotope ($\delta^{18}O_{shell}$) analysis has become the most commonly used procedure, leading to fundamental improvements of our understanding of the climate development in the Jurassic (e.g. Dera *et al.* 2011; Korte *et al.* 2015; Martinez and Dera 2015). Whereas results for different benthic taxa (e.g. bivalves and rhynchonellid brachiopods) are generally similar (e.g. Alberti *et al.* 2012*a*), belemnite rostra have often been found to record higher $\delta^{18}O_{shell}$ values than co-occurring benthic organisms (e.g. Prokoph *et al.* 2008; Mutterlose *et al.* 2010; Alberti *et al.* 2012*a*, 2019*a*). When using the same method for temperature reconstructions, this difference leads to the reconstruction of water

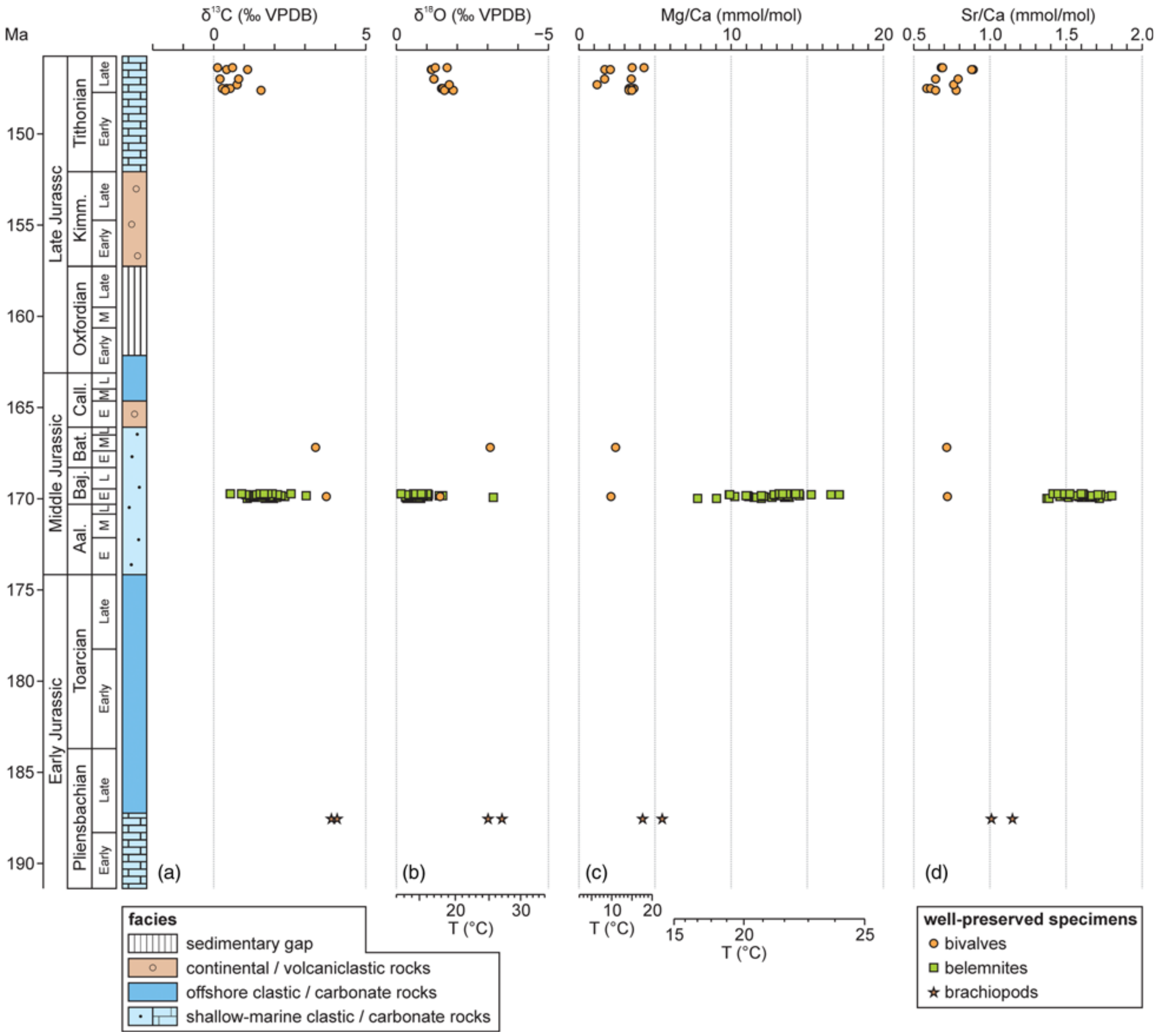

Fig. 6. Results of stable isotope ($\delta^{18}O$, $\delta^{13}C$) and element (Mg/Ca, Sr/Ca) analyses of well-preserved fossils of the southern sections near Zapala. Temperatures for $\delta^{18}O_{shell}$ values were reconstructed with the equation of Anderson and Arthur (1983) and a $\delta^{18}O_{sea}$ value of −1‰ for an ice-free Jurassic world as suggested by Shackleton and Kennett (1975). Temperatures for Mg/Ca ratios were calculated with the equations of Mouchi *et al.* (2013) for oysters and Nunn and Price (2010) for belemnites. Main facies types are based on Howell *et al.* (2005) and the age model is based on Ogg *et al.* (2016).

temperatures commonly 4–5°C lower for belemnites compared with shells of co-occurring bivalves or rhynchonellid brachiopods (also compare Dera *et al.* 2011). A series of reasons have been suggested for this seemingly systematic difference, including different life habits (e.g. a migratory behaviour of belemnites) or vital effects during the formation of the belemnite rostrum (e.g. Mutterlose *et al.* 2010; Hoffmann and Stevens 2019). Because belemnites are an extinct faunal group, deciphering all processes affecting the stable isotope composition of their hardparts is difficult. In any case, it is clear that results from belemnites should be interpreted cautiously and separately from those of benthic organisms. For Jurassic calcitic shells, absolute palaeotemperatures are most commonly calculated by the equation given by Anderson and Arthur (1983) with a $\delta^{18}O_{sea}$ value of −1‰ during shell formation (as suggested for an ice-free world; Shackleton and Kennett 1975). Following this approach, stable isotope analyses for belemnite rostra of the northern and southern sections as well as for the oysters and brachiopods of the southern sections lead to reasonable water temperatures (Figs 5 and 6). Oxfordian and Tithonian belemnites from the northern sections show a slightly higher variation indicating water temperatures between 13.1 and 20.5°C with an outlier at 30.6°C (overall average 17.8°C). The Bajocian belemnites of the southern sections indicate water temperatures between 12.6 and 18.2°C with one outlier at 25.7°C (overall average 15.2°C). As expected, the $\delta^{18}O_{shell}$ values of oysters and brachiopods of the southern sections would translate into slightly higher temperatures between 16.6 and 27.0°C (average 19.4°C). In contrast, the oysters of the northern sections near Chos Malal recorded $\delta^{18}O_{shell}$ values below −5‰, which would correspond to unrealistic temperatures of 35–60°C.

Reconstructing absolute water temperatures based on several different element ratios has become another standard method (particularly using foraminifers and corals; e.g. Eggins *et al.* 2003; Corrège 2006; McArthur *et al.* 2007; Cléroux *et al.* 2008; Hetzinger *et al.* 2016; Pfeiffer *et al.* 2017). Experiments on recent bivalve shells have shown that Mg/Ca ratios indeed reflect water temperatures and might be more independent of freshwater influence or enhanced evaporation compared with $\delta^{18}O_{shell}$ values (e.g. Klein *et al.* 1996; Bougeois *et al.* 2016). However, these studies also revealed that the exact relationship between water temperature and Mg/Ca ratio in the shell depends strongly on the examined species. Consequently, different equations for temperature reconstructions have been developed for different taxa (compare Surge and Lohmann 2008; Nunn and Price 2010; Mouchi *et al.* 2013; Tynan *et al.* 2017). Because the species used

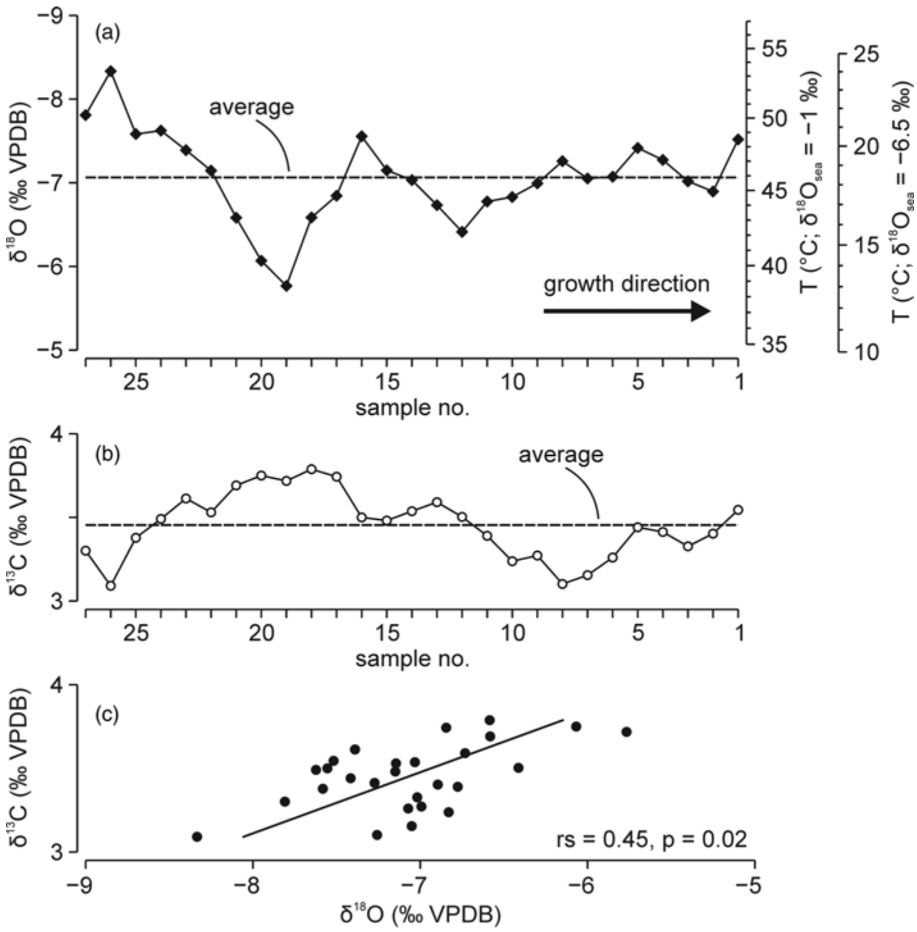

Fig. 7. (**a**, **b**) Results of high-resolution stable isotope ($\delta^{18}O$, $\delta^{13}C$) analysis of a specimen of *Gryphaea* sp. (MOZ-PI 11847/13) from the Lower Oxfordian of the Vega de la Veranada near Chos Malal. Temperatures were calculated with the equation of Anderson and Arthur (1983) and a $\delta^{18}O_{sea}$ value of −1‰ (Shackleton and Kennett 1975) and alternatively −6.5‰. (**c**) $\delta^{18}O$ v. $\delta^{13}C$ values of the oyster used for the high-resolution stable isotope analysis shows a weak positive correlation.

in the current study are long extinct, their Mg/Ca–temperature relationship cannot be measured. Consequently, all temperature reconstructions based on Mg/Ca ratios of extinct organisms should be treated cautiously. Nevertheless, although absolute temperature estimates based on Mg/Ca ratios might be unreliable, temperature trends through time might be captured with this method.

Belemnites, which do not have closely related living relatives, are especially difficult to interpret. Nunn and Price (2010) proposed an equation to translate Mg/Ca ratios of belemnite rostra into water temperatures. Using their equation, the Oxfordian and Tithonian specimens of the northern sections would indicate water temperatures between 17.2 and 23.3°C (average 19.6°C; Fig. 5c), values that are in the same range as those estimated from $\delta^{18}O_{shell}$ values. Similarly, the Bajocian specimens of the southern sections would translate into temperatures between 17.0 and 24.2°C (average 21.4°C; Fig. 6c). However, whether the Mg/Ca ratios of belemnite rostra can be used for temperature reconstructions is still debated. Whereas researchers such as Nunn and Price (2010) have found a negative correlation between Mg/Ca ratios and $\delta^{18}O_{shell}$ values in belemnites and assumed that temperatures determine the oxygen isotope and Mg/Ca ratio in the rostra (sometimes also Sr/Ca; e.g. McArthur *et al.* 2007), Li *et al.* (2013) have found no such correlation in their analyses of Jurassic and Cretaceous belemnites and concluded that this ratio is unreliable as a palaeotemperature proxy. In the current dataset, there is a weak negative correlation between $\delta^{18}O_{shell}$ values and Mg/Ca ratios of belemnites, whether examined for the entire collection ($rs = -0.35$, $P = 0.02$) or separately for specimens of the north ($rs = -0.68$, $P = 0.05$) and south ($rs = -0.32$, $P = 0.07$). At the same time, there is no correlation between $\delta^{18}O_{shell}$ values and Sr/Ca ratios of belemnites ($rs = -0.04$, $P = 0.82$; compare Supplementary material).

If the equation developed by Mouchi *et al.* (2013) for modern juvenile *Crassostrea gigas* is used for the Jurassic oysters of the Neuquén Basin, their Mg/Ca ratios translate into relatively cool water temperatures. The Mg/Ca ratios of the oyster shells of the northern sections do not vary much from the Bathonian until the Tithonian (Fig. 5c) and would indicate temperatures between 7.6 and 15.1°C with one outlier of 32.6°C in the Late Tithonian (overall average 11.5°C). Similarly, the oysters of the southern sections show relatively little variation in their Mg/Ca ratios, which would translate into temperatures between 6.4 and 18.0°C (average 12.5°C). However, these absolute temperature values depend very strongly on the equation used and there is no reason to assume that the equation of Mouchi *et al.* (2013) applies to the Jurassic species used in the present study. Nevertheless, another equation developed by Surge and Lohmann (2008) for the modern *Crassostrea virginica* in an estuarine setting leads to even colder temperatures, if applied to the present dataset. In any case, it should be noted that the Mg/Ca ratios are more or less the same for material from the northern and southern sections.

In summary, it seems that $\delta^{18}O_{shell}$ values of rhynchonellid brachiopods and oysters allow the most reliable and realistic absolute water temperature reconstructions, if the $\delta^{18}O_{sea}$ value can be approximated properly. In contrast, the $\delta^{18}O_{shell}$ values of belemnite rostra lead to an underestimation of water temperatures if following the traditional approach by using the equation of Anderson and Arthur (1983) or require the usage of a separate equation difficult to establish for this extinct group. Finally, Mg/Ca ratios are strongly dependent on species-specific fractionation factors.

The Sr/Ca ratio of seawater

Previous researchers proposed that Sr/Ca ratios of fossil hardparts reflect ancient water temperatures based on a negative correlation with $\delta^{18}O_{shell}$ values (compare McArthur *et al.* 2007; Sosdian *et al.* 2012). However, subsequent research failed to confirm a strong link between water temperatures and Sr/Ca ratios (Korte and Hesselbo 2011). Similarly, the present dataset from Argentina shows no correlation between Sr/Ca ratios and $\delta^{18}O_{shell}$ values. Instead, it seems that the ratio is largely a function of species-specific factors (e.g. fractionation factor, metabolism) and the original Sr/Ca ratio of the surrounding water body (compare Steuber and Veizer 2002; Ullmann *et al.* 2013*a*). Ullmann *et al.* (2013*a*) reconstructed Sr/Ca ratios of Jurassic seawater by using a Sr distribution coefficient of 0.10 for bivalve shells and a coefficient of 0.32 for belemnite rostra. If these coefficients are applied on the current dataset of the Neuquén Basin, the results of the northern and southern sections are similar (Fig. 8) and compare well with the proposed global seawater Sr/Ca curve compiled from data of Ullmann *et al.* (2013*a*, 2016). The results of the two Pliensbachian brachiopod shells are also comparable with the global curve if a Sr distribution coefficient of 0.32 is used. The most striking features of the curve of Ullmann *et al.* (2013*a*, 2016) are a decrease in seawater Sr/Ca ratios throughout the Middle Jurassic, a minimum in the Oxfordian, a subsequent increase in values towards the mid-Tithonian, and a slight decrease again towards the Jurassic–Cretaceous boundary. This trend is attributed to global tectonic events (Ullmann *et al.* 2013*a*) and is also similar to the global $^{87}Sr/^{86}Sr$ curve as compiled by McArthur *et al.* (2012) and Wierzbowski *et al.* (2017). Although both proxies do not have to be directly related, Ullmann *et al.* (2013*a*) suggested a common cause for the parallel fluctuations in an interplay between continental input and mid-ocean ridge activity. In any case, the current data suggest that water exchange between the Neuquén Basin and the open ocean occurred during the sampled time intervals, although both regions were separated by a volcanic arc (Fig. 1). The slightly higher absolute values could be explained by uncertainties in the Sr distribution coefficients for the fossil taxa used. Alternatively, an influx of water masses with higher Sr/Ca ratios into the basin has to be postulated. In general, modern rivers have Sr/Ca ratios lower than those of modern oceans (e.g. Sosdian *et al.* 2012) except for some arid regions in which riverine Sr/Ca ratios can be up to 16.0 mmol mol^{-1} (Holmden and Hudson 2003).

The $\delta^{18}O$ value of seawater

Reconstructions of absolute water temperatures based on $\delta^{18}O_{shell}$ values of fossil hardparts require knowledge of the $\delta^{18}O_{sea}$ value. Most studies focusing on the Jurassic time interval use a $\delta^{18}O_{sea}$ value of −1‰ to acknowledge the lack of polar ice shields (Shackleton and Kennett 1975). In general, this is an oversimplification that neglects a likely latitudinal gradient in $\delta^{18}O_{sea}$ values, with considerably higher values in the tropics and lower values at high latitudes, caused by the hydrological cycle (compare Zachos *et al.* 1994; LeGrande and Schmidt 2006; Roche *et al.* 2006). However, the Neuquén Basin was situated at a palaeolatitude of *c.* 40°S throughout most of the Jurassic (Besse and Courtillot 2002; Torsvik *et al.* 2012; van Hinsbergen *et al.* 2015), which corresponds approximately to the point where the latitudinal $\delta^{18}O_{sea}$ gradient could have reached a value of −1‰ (compare Alberti *et al.* 2020). Thus, using this value in the equation of Anderson and Arthur (1983) leads to the reconstruction of reasonable water temperatures for the studied well-preserved belemnites, as well as the oyster and brachiopod shells of the southern sections. In contrast, the $\delta^{18}O_{shell}$ values of the bivalves from the northern sections are very negative and would correspond to very high, unrealistic water temperatures. Several options are theoretically possible to explain such negative $\delta^{18}O_{shell}$ values, which will be discussed below (compare Fig. 9).

(1) Possibly the simplest explanation for very negative $\delta^{18}O_{shell}$ values in any fossil record is a poor preservation of the analysed specimens, as diagenetic alteration generally leads to a shift of $\delta^{18}O_{shell}$ values to more negative values. However, as described above, no signs of pronounced alteration are present in the oyster shells used in this study. Furthermore, the presence of cyclic changes in $\delta^{18}O_{shell}$ values in the oyster used for high-resolution stable isotope analysis (Fig. 7) does not support strong diagenetic alteration, which would have most probably led to a more uniform stable isotope composition throughout the shell. Consequently, alteration seems to be an unlikely cause for the documented negative $\delta^{18}O_{shell}$ values of bivalves from the northern sections.

(2) If diagenetic alteration is ruled out as a possible factor and average water temperatures between 20 and 25°C are assumed for the Middle to Late Jurassic, the very negative $\delta^{18}O_{shell}$ values would correspond to $\delta^{18}O_{sea}$ values for the northern study areas (i.e. the northern–central Neuquén Basin) of −7 to −6‰ in the Bathonian to Early Oxfordian and −5 to −4‰ in the Tithonian. Such low $\delta^{18}O_{sea}$ values characterize polar waters, which are commonly enriched in ^{16}O (e.g. $\delta^{18}O_{sea}$ values of −5‰ and below have been recorded in present-day high latitudes and it can be assumed that similar and lower values were possible in the Jurassic; Schmidt *et al.* 1999; Thomas and Mol 2018). Theoretically, north-bound currents along the South American west coast could have transported polar ocean

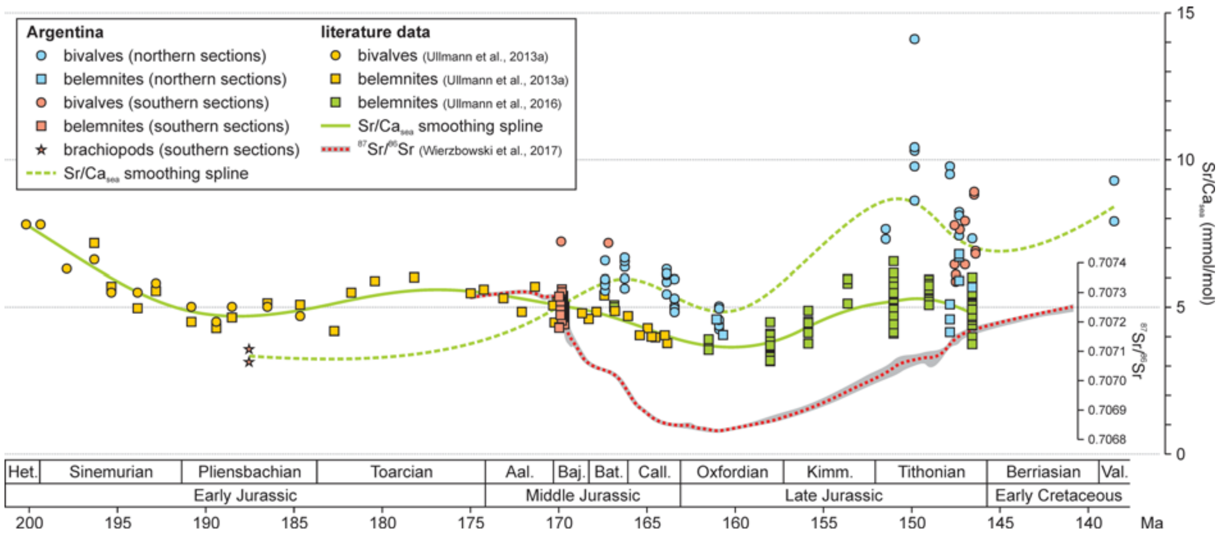

Fig. 8. Sr/Ca$_{sea}$ ratios reconstructed from fossils of the Neuquén Basin compared with data of Ullmann *et al.* (2013*a*, 2016) and the $^{87}Sr/^{86}Sr$ curve of Wierzbowski *et al.* (2017).

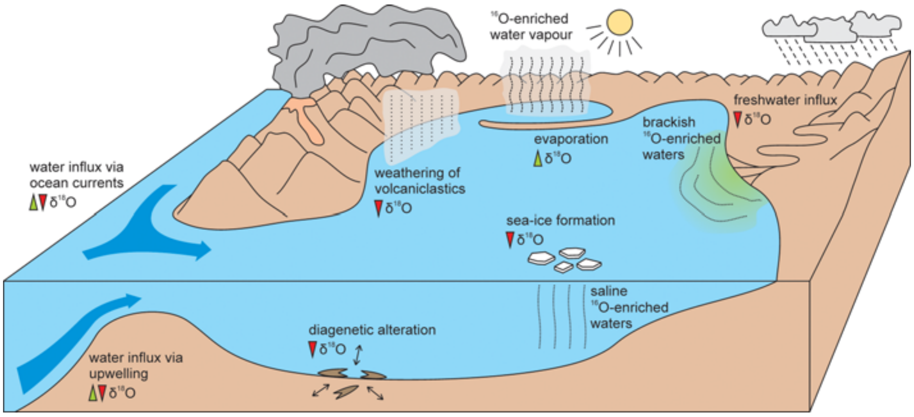

Fig. 9. Possible processes affecting the $\delta^{18}O_{sea}$ and $\delta^{18}O_{shell}$ values in marginal seas. Influx of marine waters from the open ocean can change the $\delta^{18}O_{sea}$ values positively or negatively depending on their origin. Diagenetic alteration generally leads to a decrease in $\delta^{18}O_{shell}$ values. Weathering of volcaniclastic deposits on the seafloor, sea-ice formation and freshwater influx lower $\delta^{18}O_{sea}$ values. In contrast, evaporation leads to an increase in $\delta^{18}O_{sea}$ values.

waters northwards during the Jurassic (similar to today). However, the Neuquén Basin was situated at a palaeolatitude of 40°S during the Middle and Late Jurassic and it seems unlikely that ocean currents could transport a negative $\delta^{18}O_{sea}$ signal so far to the north. In fact, models for absolute $\delta^{18}O_{sea}$ values in the Cretaceous do not predict particularly low values at comparable latitudes in the southern hemisphere (Zhou *et al.* 2008). Danise *et al.* (2020) described the Jurassic temperature development of the Sundance Seaway of northwestern North America. In this region (at a palaeolatitude of *c.* 40°N), Middle Jurassic oysters with very negative $\delta^{18}O_{shell}$ values were explained by an influx of Arctic waters into the epicontinental basin. The palaeogeography of the Sundance Seaway with only one connection to the open ocean at high latitudes in northern North America is relatively well known. In contrast, the extent to which the volcanic arc separated the Neuquén Basin from the open ocean is still debated (Fig. 1). Some palaeogeographical reconstructions indicate a rather loose chain of islands, which would allow water exchange through a series of channels west of the actual basin (e.g. Spalletti *et al.* 2000, fig. 8; Howell *et al.* 2005, fig. 4). Similarly, the Sr/Ca ratios measured for the current study point to water exchange with the open ocean during the studied time intervals (see above). In contrast, Scherer and Goldberg (2007, fig. 1) seemed to imply that the main connection to the open ocean was situated at high latitudes in southern South America. However, if an influx of polar waters from the south into an otherwise restricted Neuquén Basin is used to explain the very negative $\delta^{18}O_{shell}$ values of the oysters from the northern sections, it seems unclear why the remaining fossils do not show similar values. Furthermore, Vicente (2005, fig. 13; 2006) proposed that the major connection of the Neuquén Basin with the open ocean was actually situated in the north (i.e. the Curepto Strait; Fig. 1b) and the basin might have been closed towards the south (also compare Howell *et al.* 2005, fig. 4; Parent 2006; Kietzmann *et al.* 2014, fig. 1; Godoy 2015, fig. 2). It might be speculated that upwelling along the South American west coast could bring polar water masses with low $\delta^{18}O_{sea}$ values into the Neuquén Basin. Although seasonal upwelling along western South America has been predicted by some Jurassic climate models (Price *et al.* 1995), no evidence for this process has been found in the studied sediments, fossil faunas or geochemistry (e.g. Li enrichments in shells; Sadatzki *et al.* 2019).

(3) The formation of sea ice leads to water masses with higher salinities and lower $\delta^{18}O_{sea}$ values that sink to the seafloor (compare Barrera *et al.* 1987; Ravelo and Hillaire-Marcel 2007). However, at a palaeolatitude of 40°S for the Neuquén Basin in the Middle and Late Jurassic, the formation of extensive sea ice is very unlikely (although some Jurassic climate models suggest sub-zero temperatures at comparable palaeolatitudes in India; Sellwood *et al.* 2000). Furthermore, changes in $\delta^{18}O_{sea}$ values via sea ice formation would be only seasonal.

(4) The breakdown of volcaniclastic deposits into smectite and mixed layer clays at the sediment–water interface and/or within the sediment can lower $\delta^{18}O$ values by several per mil in bottom water and porewaters (Lawrence *et al.* 1979; Price and Sellwood 1997). The existence of an active volcanic arc allowed a continuous supply of volcaniclastic deposits into the Neuquén Basin. However, it is not clear why this process should affect only the northern study areas. Furthermore, this geochemical process alone is not strong enough to cause the proposed negative $\delta^{18}O_{sea}$ values.

(5) Freshwater is generally enriched in ^{16}O and is commonly used to explain negative $\delta^{18}O_{sea}$ values. River discharge or strong rainfalls modify $\delta^{18}O_{sea}$ values particularly in surface waters, because freshwater forms lenses on top of the heavier saline water. Such freshwater influence restricted to the northern study areas could explain the very negative $\delta^{18}O_{shell}$ values of the bivalves. Meso- to brachyhaline conditions (salinities 16–20) in the Bathonian, Late Callovian and Early Oxfordian would correspond to $\delta^{18}O_{sea}$ values of −7 to −6‰ at average water temperatures of 20°C (based on the method of Lazo *et al.* 2008, fig. 3). The proposed $\delta^{18}O_{sea}$ values of −5 to −4‰ for the Tithonian would correspond to brachyhaline conditions (salinities 23–27). Whereas oysters are generally tolerant towards fluctuations in salinities and live in marine as well as brackish habitats, ammonites and belemnites are considered stenohaline. However, because these cephalopods are active swimmers, they might have migrated throughout the basin and did not necessarily live within the presumably brackish waters in the northern study areas. Separate habitats would explain the higher $\delta^{18}O_{shell}$ values of the belemnites from the northern sections. Post-mortem drift of cephalopod shells over long distances is also not unlikely.

Climate models for the Jurassic of South America predict the position of the Intertropical Convergence Zone towards the north of the Neuquén Basin (Scherer and Goldberg 2007). Although the area of the basin itself was situated in a dry region (e.g. Volkheimer *et al.* 2008), rainfall towards the north of the basin might have occurred regularly and fuelled rivers draining into the northern Neuquén Basin. Because palaeolatitudes did not change markedly during the Middle and Late Jurassic, such a situation might have been stable for long time intervals. Because very low $\delta^{18}O$ values are limited to the northern sections, this area might have been more restricted than the southern part. This is supported by the presence of two thick evaporitic units in the northern–central Neuquén Basin (Fig. 3). During these phases, the Curepto Strait must have been closed (as suggested by Vicente 2005) and the northern basin was thus separated from the open ocean (owing to sea-level changes and local tectonic movements; Hallam 2001). Lazo *et al.* (2008; see also Aguirre-Urreta *et al.* 2008) studied the stable oxygen isotope composition of Early Cretaceous oysters in the northern–central Neuquén Basin north of Zapala and near Chos Malal. Similar to the Jurassic data from this study, their results include very negative

$\delta^{18}O_{shell}$ values. Those researchers explained these values by freshwater influence in the basin during certain intervals in the Cretaceous. It seems therefore reasonable to propose salinity fluctuations in the sampled northern–central Neuquén Basin throughout the Jurassic and Cretaceous as a result of an interplay between changing river influx and seawater exchange leading either to brackish conditions or the formation of evaporites. Such a scenario changes the general understanding of the northern–central Neuquén Basin somewhat as this area was originally considered to represent a more distal and deeper area. Although the Tithonian is dominated by fine-grained sediments possibly deposited below wave base, the Bathonian to Oxfordian strata sampled here commonly show cross-bedded horizons, which cannot be deposited at great water depths. Interestingly, the $\delta^{18}O_{shell}$ values of bivalves are less negative in the Tithonian compared with the Bathonian to Oxfordian, possibly indicating a weaker freshwater influence towards the end of the Jurassic, when sea-level was generally higher.

Seasonal temperature changes

The Lower Oxfordian oyster used for high-resolution analysis shows a cyclic signal in its $\delta^{18}O_{shell}$ values interpreted to reflect seasonal patterns. However, as in other shells from the northern sections, the $\delta^{18}O_{shell}$ values are very low. Using a $\delta^{18}O_{sea}$ value of −1‰, the $\delta^{18}O_{shell}$ data would translate into unrealistic temperatures between 39 and 53°C (Fig. 7a). On the other hand, the shell's Mg/Ca ratio would indicate an unrealistically low temperature of 12.5°C by using the equation of Mouchi *et al.* (2013). If a $\delta^{18}O_{sea}$ value of −6.5‰ is applied accounting for the proposed freshwater influence, a seasonality of about 11°C is reconstructed (minimum 13.0°C, maximum 24.0°C; Fig. 7a). Because of the problems in reconstructing precise $\delta^{18}O_{sea}$ values, these absolute temperatures are less reliable. However, the temperature amplitude (= seasonality) might be in fact a reasonable estimate for the Neuquén Basin in the Oxfordian at a palaeolatitude of 40°S. In addition, fossils analysed in the present study and collected from one stratigraphic interval show a comparable variation, possibly reflecting a similarly strong seasonality (also compare ranges in results of Bowen 1963). Nevertheless, additional seasonal fluctuations in the $\delta^{18}O_{sea}$ values caused, for example, by seasonal rainfall cannot be excluded completely. In addition, the cyclic nature of the $\delta^{18}O_{shell}$ data of the oyster from Vega de la Veranada shows that the northern study areas were at least occasionally shallow enough to experience seasonal environmental changes (i.e. above the thermocline).

A synopsis of Jurassic water temperatures of South America

So far, reconstructions of absolute water temperatures for the southern hemisphere in the Jurassic are comparatively few in number. Figure 10 combines Jurassic temperature data from South America including the present dataset from the Neuquén Basin as well as results of Bowen (1963), Gómez-Dacal *et al.* (2018) and Alberti *et al.* (2019*b*).

Mg/Ca ratios of oysters and belemnites of the Neuquén Basin do not allow the reliable reconstruction of absolute water temperatures, but point to more or less stable temperature conditions throughout the studied Middle to Late Jurassic intervals. Pliensbachian brachiopods show higher Mg/Ca ratios than Bajocian and Bathonian oysters, but because the relationship between the Mg/Ca ratio and temperature differs strongly between species, it is not clear whether this decrease in values reflects a temperature decrease (Fig. 10a).

The Jurassic stable oxygen isotope record of South America (Fig. 10b) starts with data from Chile published recently by Alberti *et al.* (2019*b*). Whereas fossils near Potrerillos in northern Chile show possible freshwater influence, the specimens analysed from sections around El Transito probably recorded water temperatures (compare Alberti *et al.* 2019*b*). These shells indicate temperatures around an average of 25.9°C in the Late Sinemurian, identical to the average of 25.9°C recorded by the two Pliensbachian brachiopods of the Neuquén Basin. One brachiopod from the latest Pliensbachian of Chile might reflect the probably global Late Pliensbachian Cooling Event with a comparatively low temperature of 19.6°C (compare Alberti *et al.* 2019*b*). Late Toarcian temperatures of Chile are again relatively high around an average of 24.4°C based on brachiopod and bivalve shells. Bowen (1963) analysed seven seemingly well-preserved, but poorly dated belemnite rostra of the late Early Jurassic. A total of 30 $\delta^{18}O_{shell}$ values from the seven fossils translate into water temperatures between 12.4 and 25.3°C. The poor stratigraphic resolution somewhat diminishes the value of these temperature reconstructions. The Middle Jurassic record starts with one Bajocian oyster of the Neuquén Basin, which recorded a relatively low temperature of 17.8°C. Another oyster from the Bathonian shows again a higher temperature of 25.2°C. Middle to Late Jurassic belemnites of the Neuquén Basin analysed in the present study indicate relatively constant water temperatures around averages of 15.2°C for the Early Bajocian, 14.6°C for the Early Oxfordian and 18.7°C for the Tithonian. These values are largely comparable with results of Bowen (1963), who analysed eight samples of two belemnite rostra from the Middle Bajocian with reconstructed temperatures between 14.4 and 23.4°C. As discussed above, $\delta^{18}O_{shell}$ values of the oysters from the northern sections point to a change in $\delta^{18}O_{sea}$ values in this area, possibly caused by enhanced freshwater influence. If water temperatures between 20 and 25°C are assumed, then a $\delta^{18}O_{sea}$ value of −6.5‰ for the Bathonian to Early Oxfordian and −4.5‰ for the Tithonian can be proposed (Fig. 10b). Although $\delta^{18}O_{shell}$ values of these oysters can therefore not be used to reconstruct reliable water temperatures, the stability of Mg/Ca ratios throughout this time interval suggests the absence of major temperature changes. Oyster shells from the southern sections record water temperatures around 18.0°C in the Late Tithonian, before temperatures increase again into the Valanginian (Early Cretaceous) with two oysters pointing to temperatures around 23.2°C. Gómez-Dacal *et al.* (2018) analysed Tithonian to Valanginian oyster shells from three sections in the northern–central Neuquén Basin with results matching the present data comparatively well (Fig. 10b). Tithonian oysters of Gómez-Dacal *et al.* (2018) show a wide variability in $\delta^{18}O_{shell}$ values translating into water temperatures between 20.0 and 33.4°C (for a $\delta^{18}O_{sea}$ value of −1‰), possibly reflecting freshwater influence on some of the shells. During the Berriasian, reconstructed water temperatures are more confined around an average of 23.2°C, but in the Early Valanginian values are again fairly scattered (between 21.5 and 31.7°C). These scattered values might indicate that freshwater influx in the northern–central Neuquén Basin occurred also in the Early Cretaceous. Such a scenario is also supported by Lazo *et al.* (2008), who recorded several intervals with very negative $\delta^{18}O_{shell}$ values of oysters in the Valanginian to Barremian of the northern–central Neuquén Basin and postulated lowered salinities in this area.

Other Jurassic water temperature records of the southern hemisphere

Apart from South America, research on Jurassic water temperatures at comparatively high southern latitudes has focused on James Ross Island in Antarctica, New Zealand and the Malvinas (Falkland) Plateau.

Ditchfield *et al.* (1994) analysed Jurassic and Cretaceous macrofossils from James Ross Island in Antarctica. Their collection included ammonites, belemnites and bivalves with a Tithonian age.

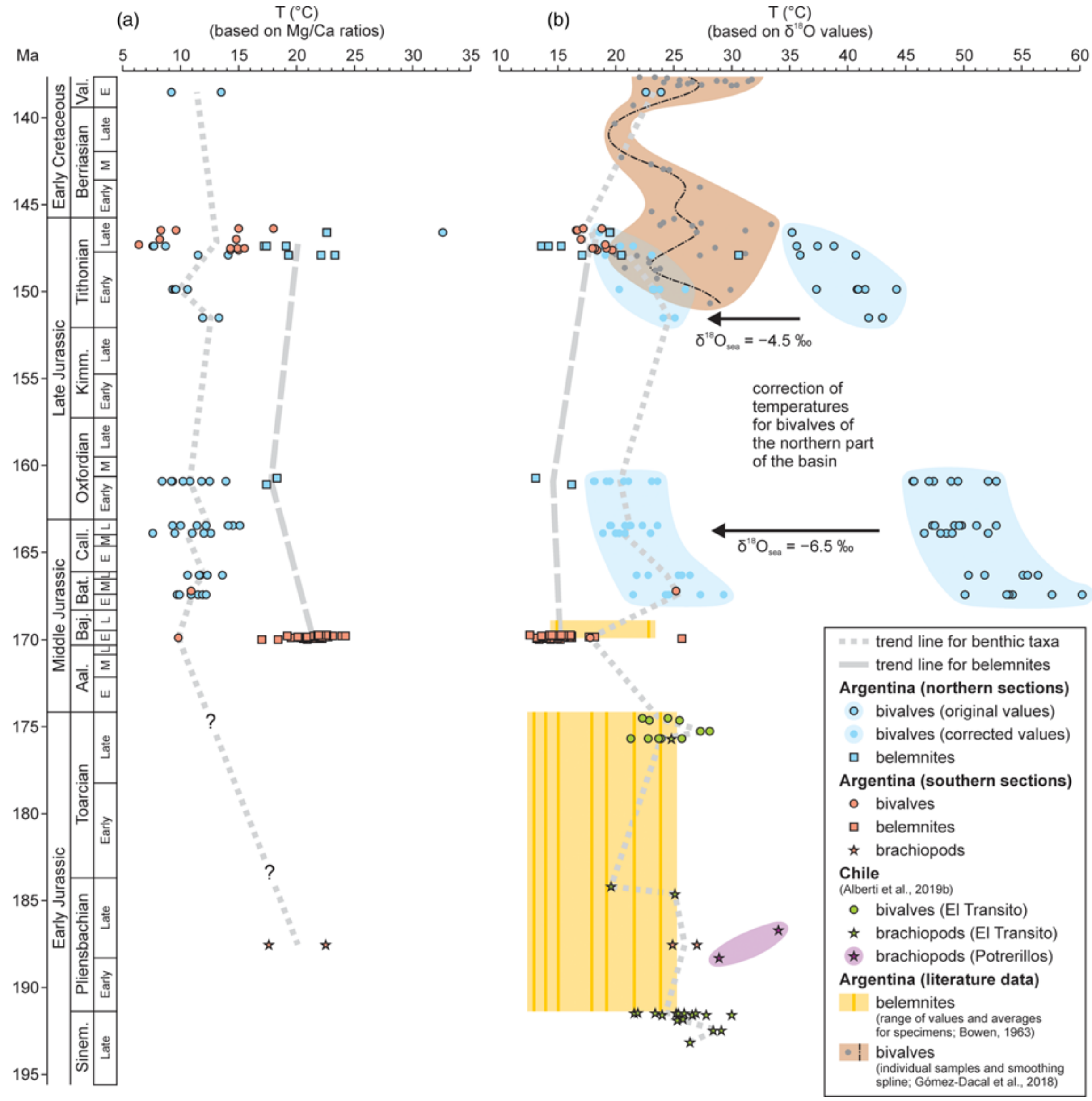

Fig. 10. Compilation of available temperature reconstructions for the Jurassic and Early Cretaceous of South America based on Mg/Ca ratios and $\delta^{18}O_{shell}$ values of bivalves, belemnites and brachiopods of Argentina and Chile (data combined from the present study and Bowen 1963; Gómez-Dacal *et al.* 2018; Alberti *et al.* 2019*b*). Temperatures for Mg/Ca ratios were calculated with the equations of Mouchi *et al.* (2013) for oysters and brachiopods and Nunn and Price (2010) for belemnites. Temperatures for $\delta^{18}O_{shell}$ values were reconstructed with the equation of Anderson and Arthur (1983) and a $\delta^{18}O_{sea}$ value of −1‰ for an ice-free Jurassic world as suggested by Shackleton and Kennett (1975). Temperatures calculated for bivalves of the northern sections were tentatively corrected by using more negative $\delta^{18}O_{sea}$ values to acknowledge a likely freshwater influence in this region. The trend lines for benthic taxa and belemnites are based on average values and serve only as orientation and broad indicators for potential long-term trends as some time intervals are not covered by data. The age model is based on Ogg *et al.* (2016).

Of these, eight belemnite rostra were considered to be well preserved and yielded $\delta^{18}O_{shell}$ values between −1.20 and −0.26‰, corresponding to water temperatures of 16.8 to 13.0°C. Ditchfield *et al.* (1994) mentioned a palaeolatitude of around 60°S for James Ross Island, but newer reconstructions point to a palaeolatitude of 45–50°S (van Hinsbergen *et al.* 2015).

Stevens and Clayton (1971) analysed belemnites from New Zealand with Bajocian to Tithonian ages at a palaeolatitude of around 80°S (van Hinsbergen *et al.* 2015). Their specimens recorded $\delta^{18}O_{shell}$ values up to 0.43‰, but also considerably lower values around −4‰ (with outliers as low as −8.5‰), some of which might be diagenetically altered. Podlaha *et al.* (1998) also analysed $\delta^{18}O_{shell}$ values of Late Jurassic belemnites of New Zealand and recorded a large variability in the results (−4.40 to 1.86‰; with one outlier at −10.99‰). Similarly, Gröcke *et al.* (2003) analysed Late Jurassic belemnites from New Zealand, noted a high variability in their oxygen ratios, and connected these to changes in the $\delta^{18}O_{sea}$ values (e.g. via the formation of ice sheets or snow) instead of strongly fluctuating water temperatures. Ullmann *et al.* (2013*b*, 2016) reconstructed water temperatures based on a large number of stable isotope analyses including Late Jurassic belemnites from New Zealand. Their specimens recorded variable $\delta^{18}O_{shell}$ values ranging between −4.1 and 0.8‰ for the Oxfordian, −3.0 and 0.5‰ for the Kimmeridgian, and −1.3 and 0.8‰ for the Early Tithonian. The highest values (up to 1.6‰) were reached in the Late Tithonian (Ullmann *et al.* 2016). Translating these values into absolute water temperatures might be difficult owing to uncertainties regarding $\delta^{18}O_{sea}$ values at very high latitudes.

Price and Sellwood (1997) analysed 26 belemnite rostra and three inoceramid bivalves with a Late Jurassic age from sites of the Deep Sea Drilling Project on the Malvinas (Falkland) Plateau. Those researchers mentioned a palaeolatitude of 55–60°S for the study area in the Late Jurassic, but more recent reconstructions point to a slightly more northern location (53–40°S; van Hinsbergen *et al.* 2015). The studied taxa recorded surprisingly negative $\delta^{18}O_{shell}$ values corresponding to very warm temperatures. Whereas Price and Sellwood (1997) argued that the inoceramids were poorly preserved ($\delta^{18}O_{shell}$ values between −2.8 and −4.2‰), they considered most of the belemnites to have a pristine composition, and explained the relatively high reconstructed water temperatures (averages for the two study areas of 17.2 and 17.9°C) by freshwater influx in the semi-enclosed basin. Price and Gröcke (2002) later analysed more Late Jurassic belemnites of the same study area with $\delta^{18}O_{shell}$ values ranging between −2.22 and −0.04‰ (translating into water temperatures of 12.1–21.2°C). Jenkyns *et al.* (2012) published TEX_{86} sea-surface temperature reconstructions ranging between 26 and 30°C for the Malvinas (Falkland) Plateau for the Middle to Late Jurassic. To explain these much warmer temperatures, Jenkyns *et al.* proposed that the analysed belemnites from the same locality lived in colder waters below the thermocline. Most recently, Vickers *et al.* (2019) used clumped isotope analyses on Late Jurassic to Early Cretaceous belemnites of the Malvinas (Falkland) Plateau and reconstructed warm temperatures between 21 and 28°C (average 25°C). In combination with $\delta^{18}O_{shell}$ values of the belemnite rostra, Vickers *et al.* reconstructed surprisingly high $\delta^{18}O_{sea}$ values of around +1‰. They explained this surprisingly high value by increased evaporation in a semi-enclosed basin.

In summary, previous stable isotope analyses of Jurassic fossils from high-latitude locations in the southern hemisphere show relatively scattered and occasionally surprisingly negative $\delta^{18}O_{shell}$ values (conventionally indicating very warm water temperatures). Similar to interpretations for the Neuquén Basin, most previous researchers have explained this by factors affecting the $\delta^{18}O_{sea}$ values (such as freshwater influence). In this regard, the present South American data match the previous records of other restricted basins very well. At the same time, some previous researchers discarded fossils with particularly negative $\delta^{18}O_{shell}$ values as poorly preserved, instead of considering other alternative explanations such as freshwater influence or lowered $\delta^{18}O_{sea}$ values of polar waters. The validity of very high temperatures reconstructed via the TEX_{86} palaeothermometer has been questioned by previous researchers (compare Vickers *et al.* 2019). Similarly, the concept of very warm temperatures reconstructed by clumped isotope analyses faces challenges. A $\delta^{18}O_{sea}$ value of +1‰ at high latitudes during the Late Jurassic should be indeed only local or regional in extent (such as in a restricted basin as proposed by Vickers *et al.* 2019). Other Jurassic temperature reconstructions for the southern hemisphere exist for the Tethys Ocean (i.e. in India and Madagascar; Fürsich *et al.* 2005; Alberti *et al.* 2012*a*, *b*, 2019*a*). These records reflect plate-tectonic movements during the rifting between western and eastern Gondwana and do not contribute to the discussion in the present study.

Conclusions

A total of 105 well-preserved belemnites, bivalves and brachiopods from two main study areas within the Neuquén Basin were analysed for their stable isotope ($\delta^{13}C$, $\delta^{18}O$) and elemental (Mg/Ca, Sr/Ca) composition. The combination of the different geochemical proxies allowed the disentanglement of different environmental parameters influencing the study area. Very negative $\delta^{18}O_{shell}$ values of oysters in the northern–central part of the basin probably reflect a variable freshwater influence (meso- to brachyhaline conditions) in this region during the Bathonian to Early Oxfordian and Tithonian. Mg/Ca and $\delta^{18}O_{shell}$ data from the remaining localities point to rather stable temperature conditions through the studied time intervals. After considering these limitations, it seems likely that water temperatures in the Neuquén Basin stayed between 20 and 25°C for most of the studied Jurassic time intervals, possibly interrupted by short colder spells in the Late Pliensbachian, Bajocian and Late Tithonian. High-resolution $\delta^{18}O_{shell}$ analysis of an oyster from the Lower Oxfordian points to a seasonality of around 11°C, if the $\delta^{18}O_{shell}$ fluctuations are explained only by temperature.

Acknowledgements The authors thank K. Bremer and V. Heinath for support with geochemical analyses, and two anonymous reviewers for their constructive criticism.

Author contributions **MA**: conceptualization (lead), funding acquisition (lead), investigation (lead), methodology (lead), writing – original draft (lead), writing – review & editing (lead); **HP**: conceptualization (supporting), funding acquisition (supporting), investigation (supporting), methodology (supporting), writing – original draft (supporting), writing – review & editing (supporting); **ACG**: conceptualization (supporting), investigation (supporting), resources (supporting), writing – original draft (supporting); **NA**: conceptualization (supporting), funding acquisition (supporting), investigation (supporting), methodology (supporting), writing – original draft (supporting), writing – review & editing (supporting); **DG**: conceptualization (supporting), funding acquisition (supporting), investigation (supporting), methodology (supporting), writing – original draft (supporting), writing – review & editing (supporting); **SD**: investigation (supporting), methodology (supporting), writing – original draft (supporting), writing – review & editing (supporting)

Funding This work was funded by the Deutsche Forschungsgemeinschaft (AL 1740/3-1).

Data availability All data generated or analysed during this study are included in this published article (and its supplementary information files).

Scientific editing by Rosalie Tostevin

References

Aberhan, M. 1994. Early Jurassic Bivalvia of northern Chile. Part I. Subclasses Palaeotaxodonta, Pteriomorphia, and Isofilibranchia. *Beringeria*, **13**, 1–115.

Aguirre-Urreta, M.B., Price, G.D., Ruffell, A.H., Lazo, D.G., Kalin, R.M., Ogle, N. and Rawson, P.F. 2008. Southern Hemisphere Early Cretaceous (Valanginian–Early Barremian) carbon and oxygen isotope curves from the Neuquén Basin, Argentina. *Cretaceous Research*, **29**, 87–99, https://doi.org/10.1016/j.cretres.2007.04.002

Alberti, M., Fürsich, F.T. and Pandey, D.K. 2012*a*. The Oxfordian stable isotope record ($\delta^{18}O$, $\delta^{13}C$) of belemnites, brachiopods, and oysters from the Kachchh Basin (western India) and its potential for palaeoecologic, palaeoclimatic, and palaeogeographic reconstructions. *Palaeogeography, Palaeoclimatology, Palaeoecology*, **344–345**, 49–68, https://doi.org/10.1016/j.palaeo.2012.05.018

Alberti, M., Fürsich, F.T., Pandey, D.K. and Ramkumar, M. 2012*b*. Stable isotope analyses of belemnites from the Kachchh Basin, western India: paleoclimatic implications for the Middle to Late Jurassic transition. *Facies*, **58**, 261–278, https://doi.org/10.1007/s10347-011-0278-9

Alberti, M., Fürsich, F.T. and Pandey, D.K. 2013. Seasonality in low latitudes during the Oxfordian (Late Jurassic) reconstructed via high-resolution stable isotope analysis of the oyster *Actinostreon marshi* (J. Sowerby, 1814) from the Kachchh Basin, western India. *International Journal of Earth Sciences*, **102**, 1321–1336, https://doi.org/10.1007/s00531-013-0864-x

Alberti, M., Fürsich, F.T., Abdelhady, A.A. and Andersen, N. 2017. Middle to Late Jurassic equatorial seawater temperatures and latitudinal temperature gradients based on stable isotopes of brachiopods and oysters from Gebel Maghara, Egypt. *Palaeogeography, Palaeoclimatology, Palaeoecology*, **468**, 301–313, https://doi.org/10.1016/j.palaeo.2016.11.052

Alberti, M., Arabas, A., Fürsich, F.T., Andersen, N. and Ziółkowski, P. 2019*a*. The Middle to Upper Jurassic stable isotope record of Madagascar: Linking temperature changes with plate tectonics during the break-up of Gondwana. *Gondwana Research*, **73**, 1–15, https://doi.org/10.1016/j.gr.2019.03.012

Alberti, M., Fürsich, F.T. and Andersen, N. 2019*b*. First steps in reconstructing Early Jurassic sea water temperatures in the Andean Basin of northern Chile based on stable isotope analyses of oyster and brachiopod shells. *Journal of Palaeogeography*, **8**, 33, https://doi.org/10.1186/s42501-019-0048-0

Alberti, M., Leshno, Y., Fürsich, F.T., Edelman-Furstenberg, Y., Andersen, N. and Garbe-Schönberg, D. 2020. Stress in the tropics? Impact of a latitudinal seawater $\delta^{18}O$ gradient on Middle Jurassic temperature reconstructions at low latitudes. *Geology*, first published online August 13, 2020, https://doi.org/10.1130/G47824.1

Anderson, T.F. and Arthur, M.A. 1983. Stable isotopes of oxygen and carbon and their application to sedimentological and paleoenvironmental problems. *SEPM Short Course*, **10**, 1–151.

Arabas, A. 2016. Middle–Upper Jurassic stable isotope records and seawater temperature variations: New palaeoclimate data from marine carbonate and belemnite rostra (Pieniny Klippen Belt, Carpathians). *Palaeogeography, Palaeoclimatology, Palaeoecology*, **446**, 284–294, https://doi.org/10.1016/j.palaeo.2016.01.033

Arabas, A., Schlögl, J. and Meister, C. 2017. Early Jurassic carbon and oxygen isotope records and seawater temperature variations: Insights from marine carbonate and belemnite rostra (Pieniny Klippen Belt, Carpathians). *Palaeogeography, Palaeoclimatology, Palaeoecology*, **485**, 119–135, https://doi.org/10.1016/j.palaeo.2017.06.007

Armella, C., Cabaleri, N. and Leanza, H.A. 2007. Tidally dominated, rimmed-shelf facies of the Picún Leufú Formation (Jurassic/Cretaceous boundary) in southwest Gondwana, Neuquén Basin, Argentina. *Cretaceous Research*, **28**, 961–979, https://doi.org/10.1016/j.cretres.2007.01.001

Armella, C., Cabaleri, N. and Leanza, H.A. 2008. Facies de patch reefs en la Formación Picún Leufú (límite Jurásico/Cretácico) en la region de Zapala, Cuenca Neuquina. *Revista del Museo Argentino de Ciencias Naturales, N.S.*, **10**, 63–70, https://doi.org/10.22179/REVMACN.10.293

Barrera, E., Huber, B.T., Savin, S.M. and Webb, P.-N. 1987. Antarctic marine temperatures: Late Campanian through Early Paleocene. *Paleoceanography*, **2**, 21–47, https://doi.org/10.1029/PA002i001p00021

Besse, J. and Courtillot, V. 2002. Apparent and true polar wander and the geometry of the geomagnetic field over the last 200 Myr. *Journal of Geophysical Research*, **107**, 2300, https://doi.org/10.1029/2000JB000050

Bougeois, L., de Rafélis, M., Reichart, G.-J., de Nooijer, L.J. and Dupont-Nivet, G. 2016. Mg/Ca in fossil oyster shells as palaeotemperature proxy, an example from the Palaeogene of Central Asia. *Palaeogeography, Palaeoclimatology, Palaeoecology*, **441**, 611–626, https://doi.org/10.1016/j.palaeo.2015.09.052

Bowen, R. 1963. O^{18}/O^{16} paleotemperature measurements on Mesozoic Belemnoidea from Neuquen and Santa Cruz provinces, Argentina. *Journal of Paleontology*, **37**, 714–718.

Brand, U. and Veizer, J. 1980. Chemical diagenesis of a multicomponent carbonate system – 1: trace elements. *Journal of Sedimentary Petrology*, **50**, 1219–1236.

Brand, U. and Veizer, J. 1981. Chemical diagenesis of a multicomponent carbonate system – 2: stable isotopes. *Journal of Sedimentary Petrology*, **51**, 987–997.

Bressan, G.S. and Palma, R.M. 2010. Taphonomic analysis of fossil concentrations from La Manga Formation (Oxfordian), Neuquén Basin, Mendoza Province, Argentina. *Journal of Iberian Geology*, **36**, 55–71.

Burckhardt, C. 1900. Profils géologiques transversaux de la Cordillère Argentino-Chilienne. Stratigraphie et Tectonique. *Annales del Museo de la Plata, Sección Geología y Minería*, **2**, 1–136.

Burckhardt, C. 1903. Beiträge zur Kenntnis der Jura- und Kreideformation der Cordillere. *Palaeontographica*, **50**, 1–144.

Carpenter, S.J. and Lohmann, K.C. 1995. $\delta^{18}O$ and $\delta^{13}C$ values of modern brachiopod shells. *Geochimica et Cosmochimica Acta*, **59**, 3749–3764, https://doi.org/10.1016/0016-7037(95)00291-7

Cléroux, C., Cortijo, E., Anand, P., Labeyrie, L., Bassinot, F., Caillon, N. and Duplessy, J.-C. 2008. Mg/Ca and Sr/Ca ratios in planktonic foraminifera: Proxies for upper water column temperature reconstruction. *Paleoceanography*, **23**, PA3214, https://doi.org/10.1029/2007PA001505

Corrège, T. 2006. Sea surface temperature and salinity reconstruction from coral geochemical tracers. *Palaeogeography, Palaeoclimatology, Palaeoecology*, **232**, 408–428, https://doi.org/10.1016/j.palaeo.2005.10.014

Danise, S., Price, G.D., Alberti, M. and Holland, S.M. 2020. Isotopic evidence for partial geochemical decoupling between a Jurassic epicontinental sea and the open ocean. *Gondwana Research*, **82**, 97–107, https://doi.org/10.1016/j.gr.2019.12.011

Dera, G., Brigaud, B. *et al.* 2011. Climatic ups and downs in a disturbed Jurassic world. *Geology*, **39**, 215–218, https://doi.org/10.1130/G31579.1

Ditchfield, P.W., Marshall, J.D. and Pirrie, D. 1994. High latitude palaeotemperature variation: New data from the Tithonian to Eocene of James Ross Island, Antarctica. *Palaeogeography, Palaeoclimatology, Palaeoecology*, **107**, 79–101, https://doi.org/10.1016/0031-0182(94)90166-X

Doyle, P. 1992. *The British Toarcian (Lower Jurassic) belemnites. Part 2. Monograph of the Palaeontographical Society*. Palaeontographical Society, London, 50–79.

Doyle, P., Kelly, S.R.A., Pirrie, D., Riccardi, A.C. and Olivero, E. 1996. Jurassic belemnite biostratigraphy of the Southern Hemisphere: a comparative study of Antarctica and Argentina. *Revista de la Asociación Geológica Argentina*, **51**, 331–338.

Doyle, P., Kelly, S.R.A., Pirrie, D. and Riccardi, A.C. 1997. Jurassic belemnite distribution patterns: implications of new data from Antarctica and Argentina. *Alcheringa*, **21**, 219–228, https://doi.org/10.1080/03115519708619175

Dromart, G., Garcia, J.-P., Picard, S., Atrops, F., Lécuyer, C. and Sheppard, S.M.F. 2003. Ice age at the Middle–Late Jurassic transition? *Earth and Planetary Science Letters*, **213**, 205–220, https://doi.org/10.1016/S0012-821X(03)00287-5

Eggins, S., De Deckker, P. and Marshall, J. 2003. Mg/Ca variation in planktonic foraminifera tests: implications for reconstructing palaeo-seawater temperature and habitat migration. *Earth and Planetary Science Letters*, **212**, 291–306, https://doi.org/10.1016/S0012-821X(03)00283-8

Epstein, S., Buchsbaum, R., Lowenstam, H.A. and Urey, H.C. 1951. Carbonate–water isotopic temperature scale. *Geological Society of America Bulletin*, **62**, 417–426, https://doi.org/10.1130/0016-7606(1951)62[417:CITS]2.0.CO;2

Fujioka, H., Takayanagi, H., Yamamoto, K. and Iryu, Y. 2019. The effects of meteoric diagenesis on the geochemical composition and microstructure of Pliocene fossil *Terebratalia coreanica* and *Laqueus rubellus* brachiopod shells from northeastern Japan. *Progress in Earth and Planetary Science*, **6**, 45, https://doi.org/10.1186/s40645-019-0289-7

Fürsich, F.T., Singh, I.B., Joachimski, M., Krumm, S., Schlirf, M. and Schlirf, S. 2005. Palaeoclimatic reconstructions of the Middle Jurassic of Kachchh (western India): An integrated approach based on palaeoecological, oxygen isotopic, and clay mineralogical data. *Palaeogeography, Palaeoclimatology, Palaeoecology*, **217**, 289–309, https://doi.org/10.1016/j.palaeo.2004.11.026

Garrido, A.C. and Parent, H. 2013. Estratigrafía y fauna de amonites de los depósitos 'Lotenianos' (Caloviano Medio-Oxfordiano Inferior?) del anticlinal de Picún Leufú, Cuenca Nequina – Subcuenca de Picún Leufú, Argentina. *Boletín del Instituto de Fisiografía y Geología*, **83**, 35–68.

Godoy, E. 2015. The north-western margin of the Neuquén Basin in the headwater region of the Maipo drainage, Chile. *Geological Society, London, Special Publications*, **399**, 155–165, https://doi.org/10.1144/SP399.13

Gómez-Dacal, A.R., Gómez-Peral, L.E., Spalletti, L.A., Sial, A.N., Siccardi, A. and Poiré, D.G. 2018. First record of the Valanginian positive carbon isotope anomaly in the Mendoza shelf, Neuquén Basin, Argentina: palaeoclimatic implications. *Andean Geology*, **45**, 111–129, https://doi.org/10.5027/andgeoV45n2-3059

Gröcke, D.R., Price, G.D., Ruffell, A.H., Mutterlose, J. and Baraboshkin, E. 2003. Isotopic evidence for Late Jurassic–Early Cretaceous climate change. *Palaeogeography, Palaeoclimatology, Palaeoecology*, **202**, 97–118, https://doi.org/10.1016/S0031-0182(03)00631-X

Gulisano, C.A. 1992. Palaeogeographic evolution of west–central Argentina. *In*: Westermann, G.E.G. (ed.) *The Jurassic of the Circum-Pacific*. Cambridge University Press, New York, 150–151.

Hallam, A. 2001. A review of the broad pattern of Jurassic sea-level changes and their possible causes in the light of current knowledge. *Palaeogeography, Palaeoclimatology, Palaeoecology*, **167**, 23–37, https://doi.org/10.1016/S0031-0182(00)00229-7

Haupt, O. 1907. Beiträge zur Fauna des oberen Malm und der unteren Kreide in der argentinischen Cordillere. *Neues Jahrbuch für Mineralogie, Geologie und Paläontologie, Beilage-Bände*, **21**, 187–236.

Hetzinger, S., Pfeiffer, M., Dullo, W.-C., Zinke, J. and Garbe-Schönberg, D. 2016. A change in coral extension rates and stable isotopes after El Niño-induced coral bleaching and regional stress events. *Scientific Reports*, **6**, 32879, https://doi.org/10.1038/srep32879

Hodgson, W.A. 1966. Carbon and oxygen isotope ratios in diagenetic carbonates from marine sediments. *Geochimica et Cosmochimica Acta*, **30**, 1223–1233, https://doi.org/10.1016/0016-7037(66)90121-9

Hoffmann, R. and Stevens, K. 2019. The palaeobiology of belemnites – foundation for the interpretation of rostrum geochemistry. *Biological Reviews*, **95**, 94–123, https://doi.org/10.1111/brv.12557

Holmden, C. and Hudson, J.D. 2003. $^{87}Sr/^{86}Sr$ and Sr/Ca investigation of Jurassic mollusks from Scotland: implications for paleosalinities and the Sr/Ca ratio of seawater. *Geological Society of America Bulletin*, **115**, 1249–1264, https://doi.org/10.1130/B25204.1

Howell, J.A., Schwarz, E., Spalletti, L.A. and Veiga, G.D. 2005. The Neuquén Basin: an overview. *Geological Society, London, Special Publications*, **252**, 1–14, https://doi.org/10.1144/GSL.SP.2005.252.01.17

Howlett, P.J. 1989. *Late Jurassic–Early Cretaceous cephalopods of eastern Alexander Island, Antarctica. Special Papers in Palaeontology*, **41**. Palaeontological Association, London.

Hudson, J.D. 1977. Stable isotopes and limestone lithification. *Journal of the Geological Society, London*, **133**, 637–660, https://doi.org/10.1144/gsjgs.133.6.0637

Jenkyns, H.C., Schouten-Huibers, L., Schouten, S. and Sinninghe Damsté, J.S. 2012. Warm Middle Jurassic–Early Cretaceous high-latitude sea-surface temperatures from the Southern Ocean. *Climate of the Past*, **8**, 215–226, https://doi.org/10.5194/cp-8-215-2012

Kietzmann, D.A., Palma, R.M., Riccardi, A.C., Martín-Chivelet, J. and López-Gómez, J. 2014. Sedimentology and sequence stratigraphy of a Tithonian–Valanginian carbonate ramp (Vaca Muerta Formation): A misunderstood exceptional source rock in the southern Mendoza area of the Neuquén Basin, Argentina. *Sedimentary Geology*, **302**, 64–86, https://doi.org/10.1016/j.sedgeo.2014.01.002

Klein, R.T., Lohmann, K.C. and Thayer, C.W. 1996. Bivalve skeletons record sea-surface temperature and $\delta^{18}O$ via Mg/Ca and $^{18}O/^{16}O$ ratios. *Geology*, **24**, 415–418, https://doi.org/10.1130/0091-7613(1996)024<0415:BSRSST>2.3.CO;2

Korte, C. and Hesselbo, S.P. 2011. Shallow marine carbon and oxygen isotope and elemental records indicate icehouse–greenhouse cycles during the Early Jurassic. *Paleoceanography*, **26**, A4219, https://doi.org/10.1029/2011PA002160

Korte, C., Hesselbo, S.P., Ullmann, C.V., Dietl, G., Ruhl, M., Schweigert, G. and Thibault, N. 2015. Jurassic climate mode governed by ocean gateway. *Nature Communications*, **6**, 10015, https://doi.org/10.1038/ncomms10015

Lawrence, J.R., Drever, J.I., Anderson, T.F. and Brueckner, H.K. 1979. Importance of alteration of volcanic material in the sediments of Deep Sea Drilling Site 323: chemistry, $^{18}O/^{16}O$ and $^{87}Sr/^{86}Sr$. *Geochimica et Cosmochimica Acta*, **43**, 573–588, https://doi.org/10.1016/0016-7037(79)90166-2

Lazo, D.G. 2007. Early Cretaceous bivalves of the Neuquén Basin, west–central Argentina: notes on taxonomy, palaeobiogeography and palaeoecology. *Geological Journal*, **42**, 127–142, https://doi.org/10.1002/gj.1080

Lazo, D.G., Aguirre-Urreta, M.B., Price, G.D., Rawson, P.F., Ruffell, A.H. and Ogle, N. 2008. Palaeosalinity variations in the Early Cretaceous of the Neuquén Basin, Argentina: Evidence from oxygen isotopes and palaeoecological analysis. *Palaeogeography, Palaeoclimatology, Palaeoecology*, **260**, 477–493, https://doi.org/10.1016/j.palaeo.2007.12.008

Leanza, H.A. 1990. Estratigrafía del Paleozoico y Mesozoico anterior a los movimientos intermálmicos en la comarca del Cerro Chachil, Provincia del Neuquén. *Revista de la Asociación Geológica Argentina*, **45**, 272–299.

Leanza, H.A. 1993. Estratigrafía del Mesozoico posterior a los movimientos intermálmicos en la comarca del Cerro Chachil, Provincia del Neuquén. *Revista de la Asociación Geológica Argentina*, **48**, 71–84.

Leanza, H.A., Mazzini, A., Corfu, F., Llambías, E.J., Svensen, H., Planke, S. and Galland, O. 2013. The Chachil Limestone (Pliensbachian–earliest Toarcian) Neuquén Basin, Argentina: U–Pb age calibration and its significance on the Early Jurassic evolution of southwestern Gondwana. *Journal of South American Earth Sciences*, **42**, 171–185, https://doi.org/10.1016/j.jsames.2012.07.012

LeGrande, A.N. and Schmidt, G.A. 2006. Global gridded data set of the oxygen isotopic composition in seawater. *Geophysical Research Letters*, **33**, L12604, https://doi.org/10.1029/2006GL026011

Lena, L., López-Martínez, R. *et al.* 2019. High-precision U–Pb ages in the early Tithonian to early Berriasian and implications for the numerical age of the Jurassic–Cretaceous boundary. *Solid Earth*, **10**, 1–14, https://doi.org/10.5194/se-10-1-2019

Li, Q., McArthur, J.M., Doyle, P., Janssen, N., Leng, M.J., Müller, W. and Reboulet, S. 2013. Evaluating Mg/Ca in belemnite calcite as a palaeo-proxy. *Palaeogeography, Palaeoclimatology, Palaeoecology*, **388**, 98–108, https://doi.org/10.1016/j.palaeo.2013.07.030

Martinez, M. and Dera, G. 2015. Orbital pacing of carbon fluxes by a ∼9-my eccentricity cycle during the Mesozoic. *Proceedings of the National Academy of Sciences of the USA*, **112**, 12604–12609, https://doi.org/10.1073/pnas.1419946112

McArthur, J.M., Doyle, P., Leng, M.J., Reeves, K., Williams, C.T., Garcia-Sanchez, R. and Howarth, R.J. 2007. Testing palaeo-environmental proxies in Jurassic belemnites: Mg/Ca, Sr/Ca, Na/Ca, $\delta^{18}O$ and $\delta^{13}C$. *Palaeogeography, Palaeoclimatology, Palaeoecology*, **252**, 464–480, https://doi.org/10.1016/j.palaeo.2007.05.006

McArthur, J.M., Howarth, R.J. and Shields, G.A. 2012. Strontium isotope stratigraphy. *In*: Gradstein, F.M., Ogg, J.G., Schmitz, M. and Ogg, G. (eds) *The Geological Time Scale 2012*. Elsevier, Amsterdam, 127–144.

Mouchi, V., de Rafélis, M., Lartaud, F., Fialin, M. and Verrecchia, E. 2013. Chemical labelling of oyster shells used for time-calibrated high-resolution Mg/Ca ratios: A tool for estimation of past seasonal temperature variations. *Palaeogeography, Palaeoclimatology, Palaeoecology*, **373**, 66–74, https://doi.org/10.1016/j.palaeo.2012.05.023

Mutterlose, J., Malkoc, M., Schouten, S., Sinninghe Damsté, J.S. and Forster, A. 2010. TEX_{86} and stable $\delta^{18}O$ paleothermometry of early Cretaceous sediments: implications for belemnite ecology and paleotemperature proxy applications. *Earth and Planetary Science Letters*, **298**, 286–298, https://doi.org/10.1016/j.epsl.2010.07.043

Nelson, C.S. and Smith, A.M. 1996. Stable oxygen and carbon isotope compositional fields for skeletal and diagenetic components in New Zealand Cenozoic nontropical carbonate sediments and limestones: A synthesis and review. *New Zealand Journal of Geology and Geophysics*, **39**, 93–107, https://doi.org/10.1080/00288306.1996.9514697

Nunn, E.V. and Price, G.D. 2010. Late Jurassic (Kimmeridgian–Tithonian) stable isotopes ($\delta^{18}O$, $\delta^{13}C$) and Mg/Ca ratios: New palaeoclimate data from Helmsdale, northeast Scotland. *Palaeogeography, Palaeoclimatology, Palaeoecology*, **292**, 325–335, https://doi.org/10.1016/j.palaeo.2010.04.015

Ogg, J.G., Ogg, G.M. and Gradstein, F.M. 2016. *A concise geologic time scale*. Elsevier, Amsterdam.

Parent, H. 2006. Oxfordian and Late Callovian ammonite faunas and biostratigraphy of the Neuquén–Mendoza and Tarapacá basins (Jurassic, Ammonoidea, western South-America). *Boletín del Instituto de Fisiografía y Geología*, **76**, 1–70.

Parent, H. and Garrido, A.C. 2015. The ammonite fauna of the La Manga Formation (Late Callovian–Early Oxfordian) of Vega de la Veranada, Neuquén Basin, Argentina. *Neues Jahrbuch für Geologie und Paläontologie*, **275**, 163–217, https://doi.org/10.1127/njgpa/2015/0461

Parent, H., Garrido, A.C., Schweigert, G. and Scherzinger, A. 2013. The Tithonian stratigraphy and ammonite fauna of the transect Portada Covunco–Cerrito Caracoles (Neuquén Basin, Argentina). *Neues Jahrbuch für Geologie und Paläontologie*, **269**, 1–50, https://doi.org/10.1127/0077-7749/2013/0332

Parent, H., Garrido, A.C., Scherzinger, A., Schweigert, G. and Fözy, I. 2015. The Tithonian–Lower Valanginian stratigraphy and ammonite fauna of the Vaca Muerta Formation in Pampa Tril, Neuquén Basin, Argentina. *Boletín del Instituto de Fisiografía y Geología*, **86**, 1–96.

Parent, H., Garrido, A.C., Brambilla, L. and Alberti, M. 2020. Upper Bathonian ammonites from Chacay Melehué (Neuquén Basin, Argentina) and the chronostratigraphy of the Steinmanni Zone. *Boletín del Instituto de Fisiografía y Geología*, **90**, 1–37.

Pfeiffer, M., Zinke, J., Dullo, W.C., Garbe-Schönberg, D., Latif, M. and Weber, M. 2017. Indian Ocean corals reveal crucial role of World War II bias for twentieth century warming. *Scientific Reports*, **7**, 14434, https://doi.org/10.1038/s41598-017-14352-6

Podlaha, O.G., Mutterlose, J. and Veizer, J. 1998. Preservation of $\delta^{18}O$ and $\delta^{13}C$ in belemnite rostra from the Jurassic/Early Cretaceous successions. *American Journal of Science*, **298**, 324–347, https://doi.org/10.2475/ajs.298.4.324

Price, G.D. and Gröcke, D.R. 2002. Strontium-isotope stratigraphy and oxygen- and carbon-isotope variation during the Middle Jurassic–Early Cretaceous of the Falkland Plateau, South Atlantic. *Palaeogeography, Palaeoclimatology, Palaeoecology*, **183**, 209–222, https://doi.org/10.1016/S0031-0182(01)00486-2

Price, G.D. and Sellwood, B.W. 1997. ‘Warm’ palaeotemperatures from high Late Jurassic palaeolatitudes (Falkland Plateau): Ecological, environmental or diagenetic controls? *Palaeogeography, Palaeoclimatology, Palaeoecology*, **129**, 315–327, https://doi.org/10.1016/S0031-0182(96)00058-2

Price, G.D., Sellwood, B.W. and Valdes, P.J. 1995. Sedimentological evaluation of general circulation model simulations for the ‘greenhouse’ Earth: Cretaceous and Jurassic case studies. *Sedimentary Geology*, **100**, 159–180, https://doi.org/10.1016/0037-0738(95)00106-9

Prokoph, A., Shields, G.A. and Veizer, J. 2008. Compilation and time-series analysis of a marine carbonate $\delta^{18}O$, $\delta^{13}C$, $^{87}Sr/^{86}Sr$ and $\delta^{34}S$ database through Earth history. *Earth-Science Reviews*, **87**, 113–133, https://doi.org/10.1016/j.earscirev.2007.12.003

Ravelo, A.C. and Hillaire-Marcel, C. 2007. The use of oxygen and carbon isotopes of Foraminifera in paleoceanography. *In*: Hillaire-Marcel, C. and de Vernal, A. (eds) *Proxies in Late Cenozoic Paleoceanography*. Developments in Marine Geology, Elsevier, Amsterdam, **1**, 735–764.

Roche, D.M., Donnadieu, Y., Pucéat, E. and Paillard, D. 2006. Effect of changes in $\delta^{18}O$ content of the surface ocean on estimated sea surface temperatures in past warm climate. *Paleoceanography*, **21**, A2023, https://doi.org/10.1029/2005PA001220

Rubilar, A. 2005. Heterochrony in Middle Jurassic species of *Gryphaea* (Ostreoidea, Gryphaeidae) from southern South America. *Geologica Acta*, **3**, 185–203.

Rubilar, A.E. and Lazo, D.G. 2009. Description of *Aetostreon pilmatuegrossum* sp. nov. from the Lower Cretaceous of Argentina (Neuquén Basin), and significance of the conservative left valve morphology in oysters of the genus *Aetostreon* Bayle. *Cretaceous Research*, **30**, 727–748, https://doi.org/10.1016/j.cretres.2008.12.013

Sadatzki, H., Alberti, M. *et al.* 2019. Paired Li/Ca and $\delta^{18}O$ peaks in bivalve shells from the Gulf of Panama mark seasonal coastal upwelling. *Chemical Geology*, **529**, 119295, https://doi.org/10.1016/j.chemgeo.2019.119295

Scherer, C.M.S. and Goldberg, K. 2007. Palaeowind patterns during the latest Jurassic–earliest Cretaceous in Gondwana: Evidence from aeolian cross-strata of the Botucatu Formation, Brazil. *Palaeogeography, Palaeoclimatology, Palaeoecology*, **250**, 89–100, https://doi.org/10.1016/j.palaeo.2007.02.018

Schmidt, G.A., Bigg, G.R. and Rohling, E.J. 1999. Global Seawater Oxygen-18 Database – v1.22. https://data.giss.nasa.gov/o18data/

Schwarz, E. and Howell, J.A. 2005. Sedimentary evolution and depositional architecture of a lowstand sequence set: the Lower Cretaceous Mulichinco Formation, Neuquén Basin, Argentina. *Geological Society, London, Special Publications*, **252**, 109–138, https://doi.org/10.1144/GSL.SP.2005.252.01.06

Sellwood, B.W., Valdes, P.J. and Price, G.D. 2000. Geological evaluation of multiple general circulation model simulations of Late Jurassic palaeoclimate. *Palaeogeography, Palaeoclimatology, Palaeoecology*, **156**, 147–160, https://doi.org/10.1016/S0031-0182(99)00138-8

Shackleton, N.J. and Kennett, J.P. 1975. Paleotemperature history of the Cenozoic and the initiation of Antarctic glaciation: oxygen and carbon isotope analyses in DSDP sites 277, 279, 281. *In*: *Initial Reports of the Deep Sea Drilling Project*, **29**. US Government Printing Office, Washington, DC, 743–755.

Sosdian, S.M., Lear, C.H., Tao, K., Grossman, E.L., O'Dea, A. and Rosenthal, Y. 2012. Cenozoic seawater Sr/Ca evolution. *Geochemistry, Geophysics, Geosystems*, **13**, Q10014, https://doi.org/10.1029/2012GC004240

Spalletti, L.A., Gasparini, Z., Veiga, G., Schwarz, E., Fernández, M. and Matheos, S. 1999. Facies anóxicas, procesos deposicionales y herpetofauna de la rampa marina tithoniana–berriasiana en la Cuenca Neuquina (Yesera del Tromen), Neuquén, Argentina. *Revista Geológica de Chile*, **26**, 109–123, https://doi.org/10.4067/S0716-02081999000100006

Spalletti, L.A., Franzese, J.R., Matheos, S.D. and Schwarz, E. 2000. Sequence stratigraphy of a tidally dominated carbonate–siliciclastic ramp; the Tithonian–Early Berriasian of the southern Neuquén Basin, Argentina. *Journal of the Geological Society, London*, **157**, 433–446, https://doi.org/10.1144/jgs.157.2.433

Steuber, T. and Veizer, J. 2002. Phanerozoic record of plate tectonic control of seawater chemistry and carbonate sedimentation. *Geology*, **30**, 1123–1126, https://doi.org/10.1130/0091-7613(2002)030<1123:PROPTC>2.0.CO;2

Steuer, A. 1897. Argentinische Jura-Ablagerungen. Ein Beitrag zur Kenntnis der Geologie und Paläontologie der argentinischen Anden. *Palaeontologische Abhandlungen*, **7**, 129–222.

Stevens, G.R. and Clayton, R.N. 1971. Oxygen isotope studies on Jurassic and Cretaceous belemnites from New Zealand and their biogeographic significance. *New Zealand Journal of Geology and Geophysics*, **14**, 829–897, https://doi.org/10.1080/00288306.1971.10426336

Suero, T. 1951. Descripción geológica de la Hoja 36c, Cerro Lotena (Neuquén). *Boletín de la Dirección Nacional de Geología y Minería*, **76**, 1–67.

Surge, D. and Lohmann, K. 2008. Evaluating Mg/Ca ratios as a temperature proxy in the estuarine oyster, *Crassostrea virginica*. *Journal of Geophysical Research*, **113**, G02001, https://doi.org/10.1029/2007JG000623

Thomas, H. and Mol, J. 2018. Dissolved inorganic carbon, total alkalinity, δ^{18}O-H2O, δ^{13}C-DIC, temperature, and salinity collected from discrete bottle samples from CCGS Amundsen in the Beaufort Sea during August and September 2014. PANGAEA. https://doi.pangaea.de/10.1594/PANGAEA.886238, 2018

Torsvik, T.H., Van der Voo, R. *et al.* 2012. Phanerozoic polar wander, palaeogeography and dynamics. *Earth-Science Reviews*, **114**, 325–368, https://doi.org/10.1016/j.earscirev.2012.06.007

Tynan, S., Opdyke, B.N., Walczak, M., Eggins, S. and Dutton, A. 2017. Assessment of Mg/Ca in *Saccostrea glomerata* (the Sydney rock oyster) shell as a potential temperature record. *Palaeogeography, Palaeoclimatology, Palaeoecology*, **484**, 79–88, https://doi.org/10.1016/j.palaeo.2016.08.009

Ullmann, C.V. and Korte, C. 2015. Diagenetic alteration in low-Mg calcite from macrofossils: a review. *Geological Quarterly*, **59**, 3–20, https://doi.org/10.7306/gq.1217

Ullmann, C.V., Hesselbo, S.P. and Korte, C. 2013*a*. Tectonic forcing of Early to Middle Jurassic seawater Sr/Ca. *Geology*, **41**, 1211–1214, https://doi.org/10.1130/G34817.1

Ullmann, C.V., Campbell, H.J., Frei, R., Hesselbo, S.P., Pogge von Strandmann, P.A.E. and Korte, C. 2013*b*. Partial diagenetic overprint of Late Jurassic belemnites from New Zealand: Implications for the preservation potential of δ^{7}Li values in calcite fossils. *Geochimica et Cosmochimica Acta*, **120**, 80–96, https://doi.org/10.1016/j.gca.2013.06.029

Ullmann, C.V., Campbell, H.J., Frei, R. and Korte, C. 2016. Oxygen and carbon isotope and Sr/Ca signature of high-latitude Permian to Jurassic calcite fossils from New Zealand and New Caledonia. *Gondwana Research*, **38**, 60–73, https://doi.org/10.1016/j.gr.2015.10.010

Urey, H.C., Lowenstam, H.A., Epstein, S. and McKinney, C.R. 1951. Measurement of paleotemperatures and temperatures of the Upper Cretaceous of England, Denmark, and the southeastern United States. *Geological Society of America Bulletin*, **62**, 399–416, https://doi.org/10.1130/0016-7606(1951)62[399:MOPATO]2.0.CO;2

van Hinsbergen, D.J.J., de Groot, L.V. *et al.* 2015. A paleolatitude calculator for paleoclimate studies. *PLoS One*, **10**, e0126946, https://doi.org/10.1371/journal.pone.0126946

Vicente, J.C. 2005. Dynamic paleogeography of the Jurassic Andean Basin: pattern of transgression and localisation of main straits through the magmatic arc. *Revista de la Asociación Geológica Argentina*, **60**, 221–250.

Vicente, J.-C. 2006. Dynamic paleogeography of the Jurassic Andean Basin: pattern of regression and general considerations on main features. *Revista de la Asociación Geológica Argentina*, **61**, 408–437.

Vickers, M.L., Bajnai, D., Price, G.D., Linckens, J. and Fiebig, J. 2019. Southern high-latitude warmth during Jurassic–Cretaceous: New evidence from clumped isotope thermometry. *Geology*, **47**, 724–728, https://doi.org/10.1130/G46263.1

Volkheimer, W., Rauhut, O.W.M., Quattrocchio, M.E. and Martinez, M.A. 2008. Jurassic paleoclimates in Argentina, a review. *Revista de la Asociación Geológica Argentina*, **63**, 549–556.

Weaver, A. 1931. *Paleontology of the Jurassic and Cretaceous of West Central Argentina. Memoirs of the University of Washington*, **1**. University of Washington Press, Seattle, WA.

Westermann, G.E.G. and Riccardi, A.C. 1979. Middle Jurassic ammonoid fauna and biochronology of the Argentine–Chilean Andes. Part II: Bajocian Stephanocerataceae. *Palaeontographica Abteilung A*, **164**, 85–188.

Wierzbowski, H. 2002. Detailed oxygen and carbon isotope stratigraphy of the Oxfordian in Central Poland. *International Journal of Earth Sciences*, **91**, 304–314, https://doi.org/10.1007/s005310100217

Wierzbowski, H. 2004. Carbon and oxygen isotope composition of Oxfordian–Early Kimmeridgian belemnite rostra: palaeoenvironmental implications for Late Jurassic seas. *Palaeogeography, Palaeoclimatology, Palaeoecology*, **203**, 153–168, https://doi.org/10.1016/S0031-0182(03)00673-4

Wierzbowski, H. and Joachimski, M. 2007. Reconstruction of late Bajocian–Bathonian marine palaeoenvironments using carbon and oxygen isotope ratios of calcareous fossils from the Polish Jura Chain (central Poland). *Palaeogeography, Palaeoclimatology, Palaeoecology*, **254**, 523–540, https://doi.org/10.1016/j.palaeo.2007.07.010

Wierzbowski, H., Dembicz, K. and Praszkier, T. 2009. Oxygen and carbon isotope composition of Callovian–Lower Oxfordian (Middle–Upper Jurassic) belemnite rostra from Central Poland: A record of a Late Callovian global sea-level rise? *Palaeogeography, Palaeoclimatology, Palaeoecology*, **283**, 182–194, https://doi.org/10.1016/j.palaeo.2009.09.020

Wierzbowski, H., Anczkiewicz, R., Pawlak, J., Rogov, M.A. and Kuznetsov, A.B. 2017. Revised Middle–Upper Jurassic strontium isotope stratigraphy. *Chemical Geology*, **466**, 239–255, https://doi.org/10.1016/j.chemgeo.2017.06.015

Wierzbowski, H., Bajnai, D., Wacker, U., Rogov, M.A., Fiebig, J. and Tesakova, E.M. 2018. Clumped isotope record of salinity variations in the Subboreal Province at the Middle–Late Jurassic transition. *Global and Planetary Change*, **167**, 172–189, https://doi.org/10.1016/j.gloplacha.2018.05.014

Zachos, J.C., Stott, L.D. and Lohmann, K.C. 1994. Evolution of early Cenozoic marine temperatures. *Palaeoceanography*, **9**, 353–387, https://doi.org/10.1029/93PA03266

Zhou, J., Poulsen, C.J., Pollard, D. and White, T.S. 2008. Simulation of modern and middle Cretaceous marine δ^{18}O with an ocean–atmosphere general circulation model. *Paleoceanography*, **23**, PA3223, https://doi.org/10.1029/2008PA001596